Chapter 1: Introduction

This thesis and its associated research creates a viewshed optimization algorithm to assist a user in identifying the best location at which to place an observation tower from which to compute viewshed analyses. The algorithm permits the user to enter various parameters including the approximate location of the tower, and computes a local optimal location based on line-of-sight (LoS) analysis. Three different sampling methods popular are employed both to collect data and analyze the results. Viewsheds computed both before and after optimization allow comparison and quantitative analysis regarding the amount of visible area gained, as well as identification of where that optimization is achieved.

1.1 – Geographic Information Systems

A Geographic Information System (GIS) is a software system that allows its user to manage, display, and analyze various types of spatial data. While many programs exist to display maps or manage large databases, the true advantage of a GIS is its power to analyze spatial data in a manner to meet user needs.

The validity of any GIS analysis is contingent upon the accuracy of the data used. Reality cannot be modeled perfectly, but many steps can be taken to ensure potential sources of error are minimized. The fundamental dataset used in this experiment is a Digital Elevation Model (DEM), a raster model with values that represent continuous variation of variables across space (figure 1.1). Raster data models are often employed to represent natural phenomena (as opposed to vector models, which represent points, lines, or polygons and feature discrete values). DEMs, as do all raster data, represent variation as grids of square-shaped cells, each assigned a value representing the elevation at a particular

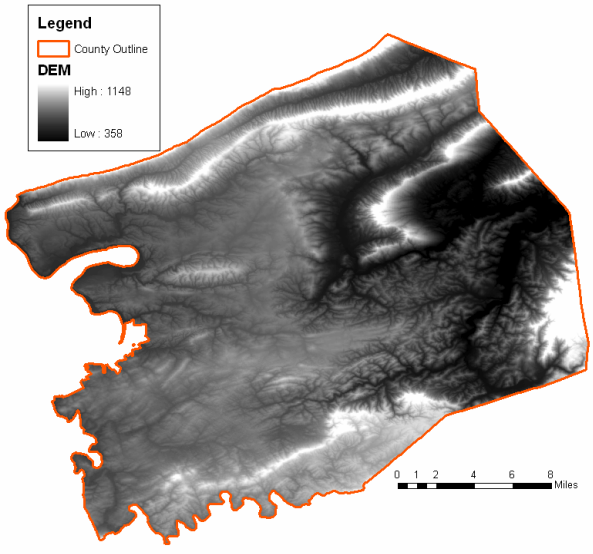

Figure 1.1 – Sample DEM for Montgomery County, Virginia

location. Increasing or decreasing the size of the cells defines the spatial resolution of the DEM and can affect both processing time and estimations of error.

1.2 – Line of Sight Analysis

A line-of-sight tool is one that determines if one point can be seen from another across a surface. Specifically, this analysis determines whether or not the surface obstructs any part of a line connecting the observation point to any given cell. Despite LoS analysis being limited to point-to-point visibility testing, it will remain a critical component of this research as discussed in section 3.3.

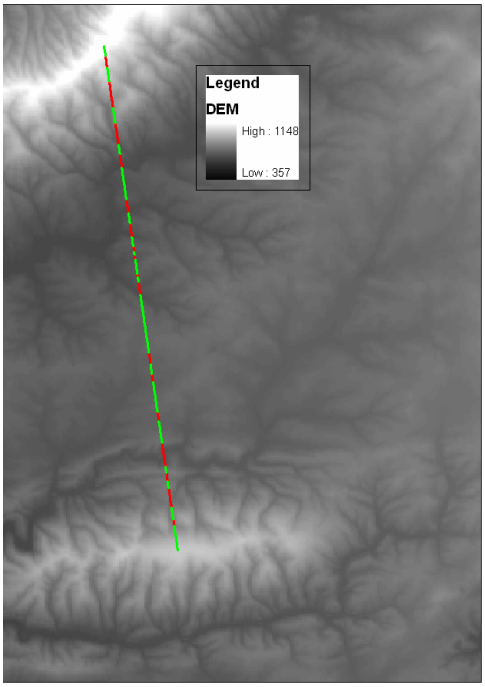

Figure 1.2 – Sample LoS. From the origin, visible points along the line in green, non visible points are red.

This research uses a customization of ArcGIS, a powerful and widely used GIS developed by Environmental Systems Research Institute (ESRI), located in Redlands, California. ArcGIS has a built-in capability to run LoS analysis in the 3D Analyst extension. While it allows for the user to input offset values above the surface (for example, to view from atop a tower or at a person's head height rather than at the level of the surface itself), customization of its algorithm is necessary to produce the desired effects for this research. Figure 1.2 provides a sample line of sight analysis using ArcGIS, extending from Brush Mountain to Price Mountain in Montgomery County, Virginia.

1.3 – Viewshed Analysis

A viewshed is defined as the set of all points visible from a particular location. It is synonymous to running a LoS analysis from one point in a DEM to every other cell to determine visibility, whereby the region or group of those final locations coded as visible comprises the initial point's viewshed.

Viewshed analysis can aid in examining many queries and solve many common geographic problems. It can determine what areas of a forest can be seen from a fire tower, assist in identifying the region covered by a cellular telephone transmitter, or show what buildings can be covered from a network of security cameras. Viewshed analysis can also be used to identify areas of low visibility when that property is desired, such as the placement of a landfill so it cannot be seen from a scenic road.

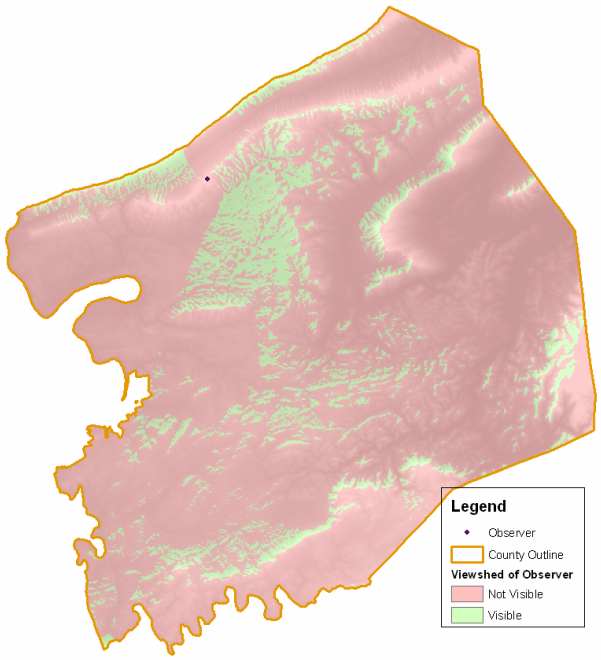

Figure 1.3 – Sample Viewshed Analysis. The area in green is visible from the observer, while pink-shaded areas are not.

ArcGIS has incorporated the capability to compute viewshed analyses in its Spatial Analyst and 3D Analyst Extensions. The tool affords great flexibility in allowing the user to enter offset values, viewing angles, and distance limits. Figure 1.3 shows a sample viewshed analysis for an observation point 10 feet above the surface atop Brush Mountain.

1.4 – Description of Study Area

The study area on which to test LoS and viewshed analyses will be the central campus of Virginia Tech in Blacksburg, Virginia. This portion of the sprawling campus is defined as the area bounded by Prices Fork Road to the North, West Campus Drive to the West, Washington Street to the South, and Kent Street and Stanger Street to the East. The study site is 7,821,793 square feet (180 acres or .28 square miles) in area. The campus ranges in elevation from 2025 feet in a pit near Derring Hall to 2191 feet atop Slusher Tower. The setting is a unique microcosm of a much larger spatial environment: while the campus is not urban in the sense of a metropolitan area, it has some of the same features as a city, such as networks of narrow pathways and a dense pattern of structures of varying heights at whose edges elevation changes abruptly. Immediately surrounding these sections of campus are open spaces with much more continuous elevation; these areas tend to be more representative of rural areas with smooth

differences in surface heights. Figure 1.4 clearly shows the pattern of open and built-up environments adjacent to each other.

Some terms used in this paper refer to distinct sections or places unique to the Virginia Tech campus, as their size, shape, or presence alters viewshed results. The 'commuter parking lot' is a large, flat parking lot that spans the entire northern section of the central campus; it is marked with an "A" on figure 1.4. The 'Drillfield' (identified with "B") is a large, oval-shaped field that roughly divides the campus in half north/south. The 'academic' or 'urban' sections of campus (marked as "C") are large sections of clustered buildings, and the small open areas, sidewalks, and roads surrounding them. There are two large academic sections of campus: one between the commuter parking lot and the Drillfield, the other between the Drillfield and the southern edge of central campus. For further information, including location and identification of all campus buildings, a detailed map of Virginia Tech's central campus can be found in Appendix D (Virginia Tech).

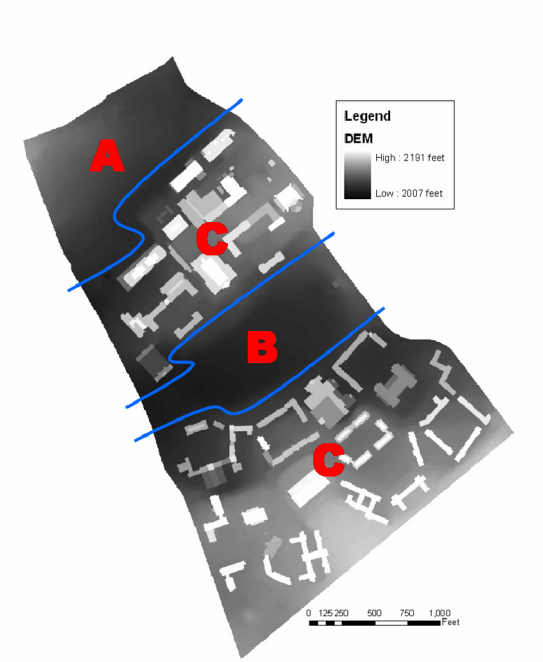

Figure 1.4 – Campus DEM and Distinct Sections Thereof

1.5 – Research Purpose, Goals, and Sampling

The purpose of this thesis is to create a viewshed optimization algorithm tool that will ultimately benefit a GIS user who chooses to employ viewsheds to create a network of cameras or sensors to provide surveillance across a region. To create such a system, a user digitizes a point in the GIS from which to compute visibility, but the location of this point is often an approximation or it may be an educated guess in the vicinity the user wants the location. With a fine resolution DEM surface, it may be impossible to find the exact top of a ridge line or slope break at which to place the tower. The first step in accomplishing the setup of a surveillance system is to allow for optimization of each individual observer; moving these observers short distances may increase the visible area in its viewshed.

The largest viewshed possible from any given point is often desirable, but commercial GIS packages offer little or no assistance in verifying whether or not another nearby location can indeed achieve a much larger viewshed than the point originally placed. The only sure method to determine the point of highest visibility in a neighborhood is to compute the viewshed for every point contained in that area, a process that is both redundant and extremely time-consuming. Instead, this algorithm will rapidly search the local neighborhood specified by the user, and through a series of computations (discussed in section 3.3), determine the optimal location. This optimal location is defined as the point that is located near the original point and contains more area visible from it than from the initial user-selected location.

It is first necessary to analyze how well the tool performs in a variety of situations. A comparison of a given point's viewsheds before and after running the optimization algorithm will indicate how much and where visible area is gained. Optimization is therefore defined as the relative percentage gain of visible area in the viewshed of the optimal location as compared to that of the initial point.

This thesis will specifically address the validity and value of the viewshed optimization algorithm by performing a different analysis for each of three sampling techniques. Samples are used when collection of data from every possible candidate is not feasible and a number of different sampling techniques are employed in research projects in nearly every discipline. The following three sampling strategies are employed:

1. Random samples are advantageous in that every location has the same probability of selection for the sample. A computer randomly generates coordinate pairs which correspond to locations in the study area, and those chosen comprise the random sample. No human interaction is involved, which limits sampling error and bias. Any patterns or clusters present in the sample data occur by chance, and therefore the locations have no true significance, allowing various spatial correlations and other statistics to be reported accurately. Additionally, analysis of individual points in the sample can identify areas of interest.

2. A transect sample is a systematic sample whereby the location for all sample points is along a linear path. Transects themselves are lines on which the sampling locations fall at regular intervals, and their presence can ensure coverage of changing space. Transect samples lend themselves to profile analysis, where measured variables are plotted across distance to see their relationships with one another over space. Specifically, graphing surface elevation and

optimization results together will show where different phenomena such as peaks or lows in optimization values occur spatially within the study area.

3. Utilization of a stratified sample is common when distinct smaller groups are present in the population. The study area is divided into several strata; each stratum's members are similar to one another in some aspect but differ from those of another. Inside each stratum, another sampling method (typically random) identifies the points to be included for the sample. This type of sample ensures adequate coverage across the entire study area. In the central campus region, different surface elevation patterns do exist, some areas are open and continuous, while others feature buildings with vertical extremes over small horizontal distances (figure 1.4). Statistical analyses of stratified samples can verify whether or not the different strata are significantly distinct, as well as determine if the variable of stratification affects its members. Comparison of viewsheds for points across different samples is not an essential component of these aforementioned examinations because each method has an advantage tailored to a distinct type of analysis.

The viewshed optimization algorithm must choose optimal locations whose viewsheds are indeed larger than those of their respective initial points, however the amount of optimization will undoubtedly vary from sample to sample. The random sample should demonstrate strong correlations among several measured variables including elevation and optimization, as an increase in the surface height should yield more viewable pixels and therefore higher optimization rates. A profile analysis with the transect sample's results should show that optimization values are highest atop buildings, but low in open areas. Similarly, the stratified sample should yield a significant distinction between the "rural" and "urban" sections of campus based on optimization results of points within the classes. The analysis of all three sampling methods is valuable in determining whether or not the viewshed optimization algorithm can be faithfully used to assist a user in placing observation locations in a viewshed analysis.

Chapter 2: Literature Review

Computing and analyzing visibility have been researched and utilized for many years, and have been facilitated by use of computerized GIS. Viewshed analyses use complex algorithms to identify areas that can be seen from an observation point and thus distinguish these areas from areas not visible (Booth 2000). User input required to compute a viewshed are a surface model representing elevation and the location of the observation point. Lines of sight (LoS) are essential to computing viewsheds, as they guide the computation and show which of their points the terrain or other obstructions hide and which are exposed.

Many theses, dissertations, and other research projects or papers have employed viewshed analyses to answer a question or solve a problem by identifying an area of high visibility. However, this research focuses on the analysis of viewsheds themselves instead of simply using them to determine the most visible area. While many have studied various aspects of the viewshed working forward (user provides viewing location to determine viewshed), research in the reverse direction (output gives viewing locations that provide maximum coverage) has not widely been examined. This chapter identifies literature relevant to this research and discusses how the contributions of others will mold the viewshed optimization algorithm and its analysis. A review of this literature yields two main classes of research.

2.1 – Different Types of Viewsheds

The most common type of viewshed analysis is a Boolean viewshed, in which the output assigns a value of 0 to cells in a DEM that cannot be seen from an observation point, and a value of 1 to those cells that can be seen. Peter Fisher, an expert and pioneer in viewshed studies, explains that the basic procedure for generating a viewshed output occurs by detecting the horizontal location at which the LoS from the viewing point to the target intersects the DEM. The elevation is then compared with the elevation of the LoS, and if the LoS elevation is higher the next intersection point is tested in the same manner. The target is said to be invisible if the surface elevation rises above the LoS. This process is then repeated for every target location in the study area (Fisher 1991). Figure 2.1 demonstrates how lines of sight are used in construction of a Boolean viewshed. Green cells indicate they are visible, red cells mean they are not. Starting with the cell in the upper left corner (visible), a line of sight analysis is performed on the

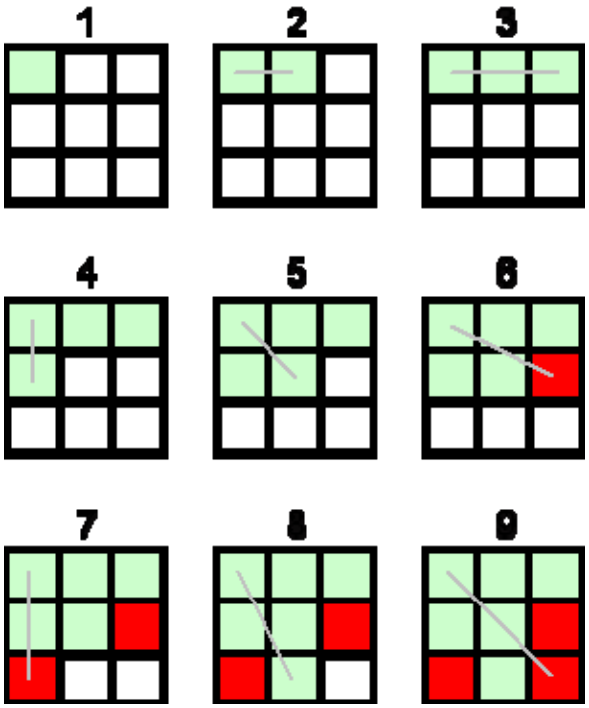

Figure 2.1 – Iterative LoS to Produce Boolean Viewshed

cell to its right (step 2). This cell is visible because there are no obstructions along the way, and it will remain visible in all future calculations. For example, step 5 concludes that the center cell is visible, so steps 6-9 illustrate this, but it had not yet been calculated in steps 1-4. The process continues, checking each other cell in the DEM.

Another type of analysis is a proportional viewshed, which is practical when there is more than one observation point, or if the observation location is not a point, but a line or area. Instead of creating an image with the values of 0 and 1, a proportional viewshed gives values in a range from 0 to 1, representing the total proportion of all observation locations that can see each location. For example, if there is a network of 50 fire towers across a vast forest, a proportional viewshed could identify the area seen by the fewest of them. If one particular cell has a value of .06, it can only be seen by three of the towers (3 / 50 = 0.06). While proportional viewsheds remain common in many similar research projects, they will not be used in viewshed optimization as the present goal is to optimize one location at a time. These analyses are very computationally intense and require large amounts of processing time.

Yet a third type of viewshed analyses is related to the proportional viewshed, but has a clear distinction. Instead of identifying whether or not an area is visible, or how visible it is, fuzzy or probabilistic analyses give the likelihood of a cell's being within view. While viewshed algorithms are inherently accurate as most error stems from the DEM, probabilistic viewsheds effectively attempt to identify those areas along borders of Boolean outputs when it is not clear whether or not a particular point is contained in a viewshed as some parameters can affect the results of a Boolean viewshed. A fuzzy viewshed is modeled by $x'_{ij} = \frac{x_{ij}}{n}$ where x_{ij} is the sum of Boolean viewshed values at row *i*, column *j* using *n* simulations. The membership function is

defined as $x' = \{0,1 : x \in X\} 0 \le x' \le 1$, meaning that the probability values lie between 0 and 1, with values closer to 1 representing those areas more likely to be visible. While the viewshed value at a particular cell is indeed a probability, the higher the value, the better it can be seen (in addition to being more likely to be seen). DEM error is simulated by the *n* simulations which produce Boolean viewsheds using the DEM with added noise values obtained from a normal distribution (Fisher 1992). The only possible values are 0 (not visible) and 1 (visible), so each time a simulated iteration finds the point visible, it raises a particular cell's value in a fuzzy viewshed when divided by the number of simulations. However, spatial analysis using fuzzy viewsheds is not common as algorithms to do so are not typically packaged in mainstream GIS software applications.

Several researchers agree with Fisher that the probabilistic viewshed is a more accurate method as error is limited and identified. Kidner et al. (2001) mention that the fuzzy viewshed is necessary as LoS prediction can be 17% worse using one DEM with a Boolean viewshed. Nackaerts et al. (1999) agree but note a drawback in that the user must determine the number of simulations used and it is necessary to run a Boolean viewshed anyways to determine possible values.

While each type of viewshed has its advantages, the selection of one must fit with a user's goals for his research. Boolean viewsheds are commonly chosen as they yield definitive yes/no visibility values, and will be utilized in this viewshed optimization project. The goal is to determine the amount of optimization possible by choosing a different starting location, and unlike other viewshed methods, a Boolean viewshed allows calculations of how much area is supposedly visible. Similarly, it allows for comparison of output irrespective of any error or fuzziness, as further discussed in section 2.2.

Other viewshed algorithms are continuously being developed but are often project specific. One such example eliminates invisible destination points by looking at the local surface's aspect and slope (Wang et al. 1996). While it employs traditional Boolean methods in concept, processing time is decreased by not having to conduct LoS analysis to every other point in the DEM. However, similar to the viewshed optimization algorithm that will be developed for this research, the means to accomplish their goals are not commercially available.

In 1993, Fisher discussed a need for standardization of viewshed operations in different GIS programs. While differences in software through algorithms and user modifications can

result in different viewshed outputs, all may still be defendable since viewsheds cannot be perfectly defined by today's GIS models. However, because different possible viewsheds are an unacceptable result, admission of error and fuzziness may make the proportional method better as it produces a likelihood image.

2.2 – Error in Viewshed Analysis

Fisher (1991) and Nackaerts et al. (1999) both mention that any viewshed must be interpreted with caution because all DEMs inherently contain many inaccuracies. Error is immediately introduced to the surface due to digitizing, aerial photo distortion, and projection among other sources. In their accuracy assessment of viewsheds, Nackaerts et al. find DEM error so invasive of results that they ignore it completely. This concept appears to be universally employed (Wang et al. 1996, Franklin and Vogt 2004) as error is difficult to detect and almost impossible to eliminate. Franklin and Vogt (2004) also ignore earth curvature even though over large distances the surface can block area behind it when a map or GIS does not. Over small areas however, such as the Virginia Tech campus, earth curvature is so minimal that it does not impede viewshed accuracy, and it will not be considered in the viewshed optimization program. Although the error is present, many concede that the viewshed algorithms yield very little error themselves; viewsheds are accurate given their DEM input.

While many analyses of error in a GIS focus on digitizing, generalization, and attribute values, Ruiz (1997) noted that error in a viewshed can come from two sources: the DEM, and the landscape of the study region. Further complicating the issue is that the root mean square error (RMSE) gives only the overall amount of error in the DEM, but little can be done to identify where the error is located throughout the region. This error exhibits no spatial autocorrelation (Monckton 1995), which means its location is distributed randomly throughout a study region. By comparing a control DEM (assumed to be free of error) and a DEM attained from the United States Geological Survey (USGS) via an overlay operation, Ruiz concludes that only 80% of the total cells are classified the same (either visible or non-visible) in both DEMs. Non-visible areas tended to be correctly identified at a higher rate than their visible counterparts (Ruiz 1997).

Several have concluded that areas of high elevation generally have less error than lower areas (Ruiz 1997, Fisher 1991). Ruiz's study additionally addresses terrain ruggedness, tree coverage, and elevation and their roles in contributing to viewshed error. Some interesting

findings are that: the DEM is more likely to shield places from view when the observer height is lower, that terrain roughness accounts for approximately 51% of the variation in the RMSE, and that tree coverage is not a source of much error (Ruiz 1997).

This study is of critical importance to viewshed optimization because the high amounts of error presented by Ruiz are alarming given the large number of viewshed analyses that will be conducted for this research. Unfortunately, possible solutions for reducing error are not typically reported. For example, while tree coverage may have a role in obstructing ground and therefore causing a viewshed algorithm to predict visibility, there are many considerations as to how a DEM should model a tree. This means that after computing all viewsheds for both initial and optimal locations in this experiment, error will still be scattered throughout the entire campus, and there is no method of distinguishing areas with low amounts of error from those prone to error. Nevertheless, the same errors are present in this optimization experiment in each analysis performed as the same DEM is used throughout.

Error induced by the data structure is the focus of another study examining error in viewshed analysis. Any DEM is structured in a manner that it contains a finite number of cells, but the purpose of a viewshed is often to determine point-to-point visibility. One of the cells in the DEM contains the desired point, but if the DEM resolution is large enough, there will be variation of visibility within any one cell. The study finds that geometric principles prohibit viewshed analyses to be error free, but those cells with partial blockage can be identified as sources of error induced by data structure (Sorensen and Lanter 1993). While certainly an interesting study, a DEM for the central campus area with a resolution of 1 foot should greatly minimize results from the data structure.

2.3 – Additional Relevant Literature

Lee (1994) introduces the related concept of visibility dominance, referring to the phenomenon when all visible pixels from a viewing pixel are also visible from another viewing pixel. If pixel A's visible region is entirely included in the visible region of pixel B, pixel B dominates pixel A. Lee concludes that as elevation increases, visibility increases greatly. However, topographic features have a much greater effect on visibility dominance (Lee 1994). For example, gentle landscapes in general commonly exhibit visibility dominance because the visible pixels tend to be connected. In rugged terrain, peaks and ridges are often dominant while

pits and ravines are not. Peaks and ridges dominate and are typically at high elevations, so they are very likely candidates from which to view a large area.

This research forms an interesting component related to viewshed optimization, and its application is discussed further in section 7.2. However, as the central campus has varying topographic features representing the two classes Lee discusses, his research helps formulate the hypothesis for this thesis as well. The conclusion that varying topographic features impact visibility dominance is a key component in expecting that open areas (such as the Drillfield) will achieve little optimization because most of an initial point's neighbors can see the same area. Similarly, highly discontinuous surfaces (such as urban sections of campus) should have much higher optimization values as a neighboring pixel may be dominant as well as include much more visible area.

It is necessary for the viewshed optimization tool to both incorporate some of these ideas as well as to prove innovative. The value of this thesis will be in the usefulness of the viewshed optimization algorithm itself and the analysis of it which will determine whether or not it can be used as an effective way to site observers for viewshed analysis. With a complete understanding of the viewshed models used and the analysis of their meanings and error, this robust viewshed optimization tool will surely accomplish its intended goal.

Chapter 3: The Viewshed Optimization Algorithm

3.1 – Algorithm Information

This section addresses both the design and employment of the viewshed optimization algorithm. The program was designed specifically for situations in which it is desirable to identify the point in a local neighborhood with the highest visibility. A number of data validation techniques are incorporated into the optimization algorithm to eradicate error not already inherent in the DEM by alerting the user if an illegal value has been entered in one of the dialog fields.

Figure 3.1 – Screen Capture of Viewshed Optimization Algorithm

The algorithm first imports the DEM into the open ArcMap window, places it in the list of layers, and assigns a stretched symbolization covering the range of elevation values. The user form is then opened for the user to enter the parameters listed above. Figure 3.1 indicates what is displayed on the user's screen when running the viewshed optimization algorithm; the parameters the user can modify are discussed in section 3.2. When the user clicks the RUN button, the algorithm then begins in earnest and is effectively divided into two different procedures: that which indicates which cells to select en route from the starting location to a random point, and that which tests visibility between the two points.

3.2 – Algorithm Input

The algorithm has seven different parameters the user must enter:

1. **DEM** – indicates the surface model on which to run the algorithm.
2. **Start (*i*,*j*) coordinates** – the coordinates of the original tower placement to be optimized. (*i*,*j*) is the notation used in raster environments instead of the related

(x,y) of common Cartesian coordinate systems. i values represent columns, or horizontal distance from the origin, while j values represent rows, or vertical distance from the origin. (i,j) = (0,0) at the upper-left corner of the DEM.

3. **Neighborhood Size** – The distance, measured in rows and columns, for which the algorithm will search for the optimal observer location in the four cardinal directions. The neighborhood is a square and has sides of length ($2n$ + 1) where n equals the user input for this parameter. Figure 3.2 defines the local neighborhood where the input value is 3, creating a 7x7 neighborhood around the initial location (orange).

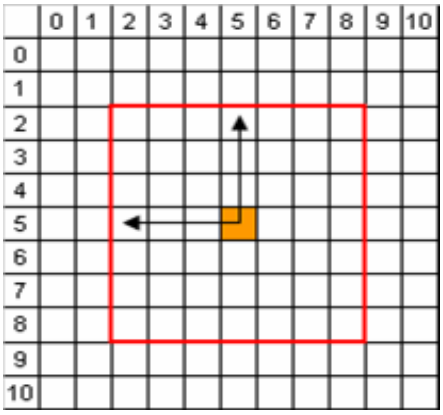

Figure 3.2 – Illustration of Neighborhood

4. **Number of Random Points** – The number of random "end" points to which to conduct a LoS visibility test from every cell in the neighborhood.
5. **Random Search Distance** – The distance limit, measured in the same units as the DEM, to which a random point can be chosen when testing for intervisibility.
6. **Observer Height** – Distance, measured in the same units as the DEM, above the surface from which to compute visibility.
7. **Output File** – Full path and name of text file where the visibility statistics will be stored.

3.3 – Algorithm Process

The program begins at the upper-left corner of the square-shaped neighborhood around the starting cell. For example, if the starting cell is (500,500), and the neighborhood value is defined as 4, the procedure begins at (496,496). From there, it chooses a random point within the specified random distance, and follows a modified version of the Bresenham algorithm to determine which cells to select to arrive at the random point (Bresenham 1965). If the line connecting the starting cell and the random point has a slope greater than 1 (slope steeper than the line y = x), the algorithm chooses cells along the way so that no j coordinate can be repeated.

Similarly, if the line connecting the starting cell and the random point has a slope less than 1 (slope shallower than the line y = x), the algorithm chooses cells along the way so that no *i* coordinate can be repeated. The Bresenham component keeps track of several variables along the way to determine when to switch to the next *i* (for steeper slopes) or to the next *j* (for shallower slopes). Figure 3.3 demonstrates the path that the Bresenham line algorithm follows to connect the initial location (1,1) and the final location (9,5). The initial and final locations are shaded in dark orange.

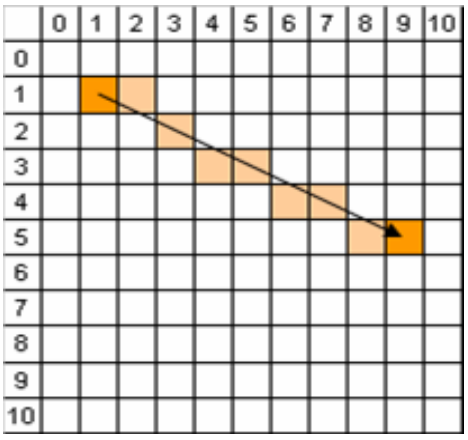

Figure 3.3 – Illustration of Bresenham Algorithm

As each sight line is computed by the Bresenham algorithm, the program tests for LoS visibility along that line. To calculate intervisibility, the LoS elevation is computed, along a line that connects the observation tower from the random ending cell. The elevation at the random ending cell is subtracted from the sum of the elevation at the starting cell plus the user-specified tower height (end cell elevation – (start cell elevation + tower height)). This elevation difference divided by the distance between the two points represents the slope of the LoS elevation line, and at every cell along the way is multiplied by an integer counter indicating how far along the line a particular cell is located (so that at the end of the line, the counter equals the length of the line). The LoS elevation is compared with the surface elevation at every cell along the line between the starting cell and the random ending point. Figure 3.4 shows visible surface in green and non visible surface in red from the blue observation point. From the observer to any location on the surface, the ground is always visible unless one of the lines of sight (gray) intersects any surface before it.

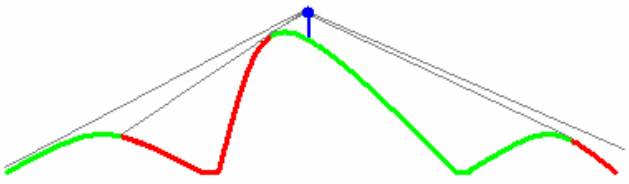

Figure 3.4 – Illustration of LOS and Surface Elevations

So long as the value of the LoS elevation line is greater than the surface elevation at every cell along the line produced by the Bresenham algorithm, the end cell is visible from the start cell. Once the procedure arrives at the random ending point, it repeats itself using a different random point until it has iterated to the number of random points specified by the user, at which point it begins at the next starting cell,

looping until the procedure has been repeated for all cells within the neighborhood specified by the user. However, if at any point along the line the surface elevation is greater than that of the LoS elevation, anything beyond that point is invisible from the starting cell. In this case, because it is only desirable to know whether or not the final cell is visible from the observer location, the algorithm quits this subroutine and begins the next random ending point.

A visibility counter keeps track of how many randomly selected end cells are visible from each starting location. These numbers are compared to find the point of maximum visibility, identified by having the maximum number of random end cells categorized as visible. A text file is generated that displays how many visible random points there are from each starting location. It also identifies the point(s) of maximum visibility (depending if there is a tie in the number of random ending points visible), representing the optimal location in the local neighborhood at which to place the observation tower.

3.4 – Sample Code

The following pseudocode represents how the algorithm operates procedurally. Although pseudocode inherently does not include detailed syntax, it provides a helpful visualization of the program's structure.

```
For i = left side of the neighborhood to right side of the neighborhood
    For j = top of the neighborhood to bottom of the neighborhood
        Do until the number of random points = user specification
            Generate random end (i,j) coordinates within random distance
            For i = 1 to distance from start to end
                Select next cell in line from start cell to end cell
                Compare elevation of this cell to LoS elevation at this cell
                If surface elevation > LoS elevation Then
                    End point is not visible
                    GoTo Next random end point for testing
                Else
                    Point is visible so far
                    Continue along this line
```

End if

Next *i*

Increment number of visible points for this starting cell

Loop

Next *j*

Next *i*

Create text file and give visibility statistics

While the algorithm is fully functional, varying the user parameters can tremendously impact the processing time. Waldo Tobler's first law of geography states that places closer together are more related than those at greater distances (Tobler 1970). Cells therefore generally have a higher probability of having other cells in the immediate vicinity included in their viewshed, with cells farther away less likely to be visible. Therefore, increasing the distance at which to search outward for an ending cell results in many of the random cells chosen to not be visible, indicating that the starting location is not in an area of high visibility. Likewise, making the search distance too short can cause many of the random cells to be identified as visible, ultimately misleading that this starting cell can see large areas. A traditional Boolean viewshed can help in setting the random search distance by showing at what distances the observer can or cannot see most other points. The distance setting should also be made with consideration for the distances that the observer is trying to view from the starting cell. For example, if a tower is supposed to see for 5 miles, then setting the random search distance at 100 feet does little relevant testing.

The Bresenham algorithm is inherently rapid as it uses integer computations, and is aided by this modified version of it which places its values in an array rather than repeating calculations across the line segment. It takes less than one second for the algorithm to compute whether or not one cell is visible from any other cell. However, it must be taken into consideration that this is a very iterative process and can repeat itself many times; if the user enters a neighborhood distance of 30 and searches for 30 random end points, the process runs 28,830 times (31 x 31 x 30).

Chapter 4: Methodology

4.1 – Data Preparation

Two data sources were brought together to form the campus DEM required to test the algorithm's ability to optimize tower locations. First, a DEM with one-foot horizontal resolution was obtained from former Virginia Tech graduate student Matt Germroth, who compiled the data for his thesis on satellite viewsheds. This surface model was created by combining 1 foot base elevation contours (vertical resolution therefore is one foot), a polygon shapefile for buildings (with their associated heights), and digitized roof ridges (Germroth 2005). However, the study area for this previous study was rectangular in shape across the Virginia Tech campus and did not completely fill the desired central campus site for this viewshed optimization study.

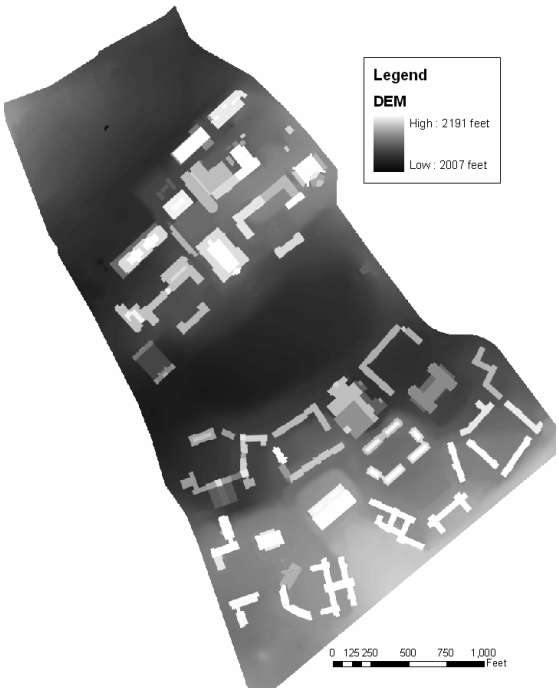

Figure 4.1 – Campus DEM used in the Experiment

To account for the missing areas and to ensure that every location in the study site had an assigned elevation value, it was necessary to collect additional data to encompass the central campus boundaries discussed in section 1.5. To achieve this, light detection and ranging (LIDAR) point elevation data was gathered from the Town of Blacksburg. The central campus and its immediate vicinity contain 9,964 points with elevation data accurate to less than one foot vertically. To incorporate this elevation data into the DEM, it was first necessary to convert the LIDAR points to a raster grid. This was accomplished by running an inverse distance weighted (IDW) algorithm, making the output cell size 1 foot to match the other DEM. IDW is a method of interpolation that assigns values to a raster at locations without an observation by using distances to locations with an observation, with shorter distances having more control over points farther away. With a dense distribution of points for interpolation, IDW yields a fairly accurate surface model (Watson and Philip 1985). The resulting raster was a surface DEM using the LIDAR data and because there were no

buildings or other obstructions within the areas not originally covered, the DEM was combined with the initial surface model using a mosaic operation (first covers second). The only other operation required to prepare the DEM for data collection was to create a copy of the DEM using the central campus boundary as an analysis mask. The final DEM now completely covered the study area clipped to the extent of the boundary so that data outside of the central campus could not be included in any analysis. Figure 4.1 shows this complete DEM.

4.2 – Input Parameter Values

Several parameters were set in order to run the viewshed optimization algorithm. Their definitions and roles were discussed in section 3.2, but their values must be justified for use in this project. The neighborhood was constructed so that the algorithm searched a distance of 30 feet in all four cardinal directions from the starting cell, as it is undesirable for the neighborhood to be too large, maximizing its distance from the original location (42.4 feet diagonally in a 61 feet x 61 feet neighborhood), and therefore not truly optimizing the initial location. For example, if a user selected a cell on the in the Virginia Tech commuter parking lot (elevation 2046 feet), with an excessively large search distance, the algorithm would have determined the best place to site the tower was atop Slusher Hall, a residence hall near the Drillfield (elevation 2177 feet). This would not really be indicative of a local solution as the building is both far away from the initial location and not representative of its immediate environment. The value was set to restrict the algorithm from searching within a range so far away that the solution is not local, yet at the same time a starting location near a building may take advantage of its proximity. As the average distance between neighbors in a sample of 50 buildings on campus averaged 58 feet, a 30 foot neighborhood was used.

The random searching distance was set at 100 feet from the starting location. This value represented the radius of a circle around the starting location outside of which no ending point will be tested for LoS visibility. This created a candidate pool of 31,416 cells available to be chosen at random for visibility testing (where area = πr^2).

For every starting cell, the algorithm tested visibility for 30 random locations within the random searching distance. This value was high enough to both reduce the probability for ties in areas with discontinuous elevation, as well as assuring that the number of visible cells truly indicates the cell's visibility. It is assumed that a sample of 30 was large enough to represent the

population such that the proportion of visible cells was correct. Justification for using this sample size appears in section 6.4, which demonstrates that while increasing or decreasing the number of random end points from 30 may result in a different optimal location selected, its viewshed is not significantly altered.

Using the surface elevation as the height from which to test for visibility would result in very small viewsheds that are not indicative of that cell's ability to see larger areas, because locations with higher elevations in the local neighborhood of that cell would block nearly all areas beyond it on a continuous surface. Similarly, setting the observation tower height too high was equally undesirable as every increase in height tends to also increase visibility. For example, in a fire tower siting study, it would not be practical to build a tower 1,000 feet high, even if at such an elevation an entire forest could be seen. For this study, a 6 foot observation tower height was used for every viewing location, representing a typical human height. The viewshed optimization algorithm has been created to search for random end points that lie on the surface.

4.3 – Resampling Process

With a one foot grid, the desired parameters search a 61x61 local neighborhood to find the optimal location. For each of these 3,721 cells, the optimization algorithm will conduct 30 LoS visibility tests at random locations not further than 100 feet away, causing the algorithm to loop 111,630 times. However, setting the parameters to these values results in the optimization algorithm taking several hours to process; it was much more practical to use a lower-resolution DEM for the testing the program. A neighborhood filter resampling method was performed on the DEM, taking the average value of every 5x5 local neighborhood and assigning it to the new DEM, thereby enlarging the cell size to 5 feet. Figure 4.2 demonstrates how the filter is performed by taking the average of the 25 central orange cells and assigning it as the value in the corresponding location in the DEM with lower resolution.

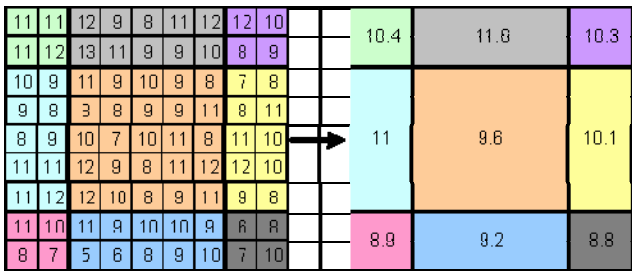

Figure 4.2 – 5x5 Neighborhood Filter

Several options were available for choosing the filtering method, including maximum value, minimum value, and average value. The DEM resampled using maximum values would

have been extremely conservative by making buildings larger and therefore reducing viewshed values. Conversely, a minimum value resampled DEM would make structures appear smaller than their actual size and cause the viewshed algorithm to incorrectly identify non visible areas as visible. Therefore, there is much risk involved, whereas there is relatively little risk using the maximum values. While using the average value in resampling did smooth out very small variations in the DEM, it was chosen as a suitable alternative to the minimum and maximum extreme options. The original was not modeled perfectly to include items such as traffic signs or mailboxes, examples of objects that would have been eliminated when using the average filter. The resampled DEM was only truly affected in five foot neighborhoods that included buildings, because over open spaces, there is little variation (with no outliers) to greatly affect the average.

The DEM was resampled because there exists a negative relationship between spatial data processing time and resolution of that data. In a study to demonstrate how fractal analysis can be used in GIS to determine scale and resolution, Lam and Quattrochi (1992) note that while accuracy does decrease with lowering resolution of spatial data, the practice is nevertheless employed in geographic research. By using a five foot DEM, the user-defined neighborhood was reduced to extending outward 6 cells to search 30 feet, just as the random search distance was reduced from 100 cells to 20 cells. The five foot grid was used solely for running the viewshed optimization algorithm. Changing the DEM resolution did not affect the scale of the z-values, so the tower height remained at 6 feet. Thus, the final user-defined parameters used in the viewshed optimization algorithm for all 80 sample starting locations were:

Neighborhood: 6

Random search distance: 20

Number of random points to test: 30

Tower height: 6

It must be noted that the purpose of this research was not to test the effect of the parameters have on the resulting optimal locations. It is assumed that while altering the values undoubtedly does affect the results, it does so in a manner consistent among all samples. Justification for using the resampled DEM appears in section 6.4 which demonstrates that processing time is greatly reduced with little effect on the resulting viewsheds.

4.4 – Data Gathering

To begin data collection, it was necessary to have different shapefiles containing the observation points for each sampling technique. Several lines of code were added in a tool which simply displays the (*i*,*j*) coordinates in the status bar in ArcMap. For the observation towers placed at random, a random number generator was used in Microsoft Excel to generate 30 *i* values between 0 and 4721 (the number of columns in the campus DEM), and 30 *j* values between 0 and 5435 (the number of rows in the campus DEM). A blank shapefile was added for this sampling technique and in editing mode, each random point was digitized in its proper (*i*,*j*) location in its respective shapefile. The campus DEM is not rectangular in shape, therefore some points added fell outside of the boundary; new points were generated in this situation to ensure all sample points were within areas containing data on the DEM. Each point was assigned a number for ease in identification. Additionally, a field was added to this vector layer's attribute table named 'OFFSETA'; its value was set to 6 (user specification) for each record. This value represented the vertical distance in surface units to be added to the z-value of the observation points, and ArcMap's viewshed process took this attribute into account when computing the viewshed.

With a shapefile including the 30 random points (locations shown in figure 4.3), a viewshed analysis was run in ArcMap's Spatial Analyst extension for each location. The input surface was the one foot campus DEM, and the observer points came from the shapefile of observation locations. The z factor was 1 (no vertical exaggeration present in the DEM), and the output raster was created with the identification number of the point serving as the file name. The resulting viewshed was a raster file with values of 0 and 1, respectively distinguishing those areas that cannot be seen from the starting cell from those that can. Displaying the histogram for the newly created viewshed layer identified how much area is in each class.

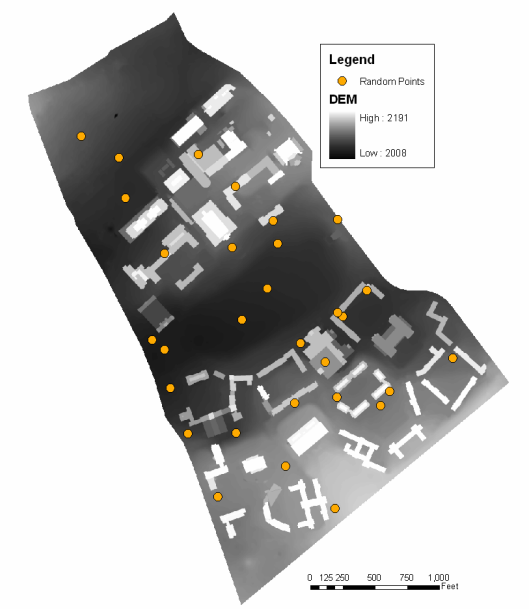

Figure 4.3 – Locations of Random Sample Points

The optimization algorithm was then run on the first starting location setting the parameters as described above in section 4.3 and using the five foot campus DEM. In a new blank shapefile, the location of the optimal observation point was digitized in the center of the 5x5 foot cell; this was repeated to have a complete shapefile of the 30 optimal locations. A viewshed output was then computed for each of the optimal locations in the manner described above, using the one foot DEM.

To identify the points used in the transect sample (shown in figure 4.4), two transect lines were drawn atop the campus DEM. To achieve this in a north/south direction, points were placed on the sections of Prices Fork Road and Washington Street that bound the study area to break each into thirds. Transect 1 connected the western-most set of points, and transect 2 connected the eastern set of points, effectively resulting in dividing the central campus area into thirds. Ten sample points were equally spaced on each of the two transects, 374 feet apart on transect 1 and 365 feet apart on transect 2. The viewshed operations for the sample points, the algorithm for optimization, and the viewsheds for the optimal points were run in the same manner as mentioned above.

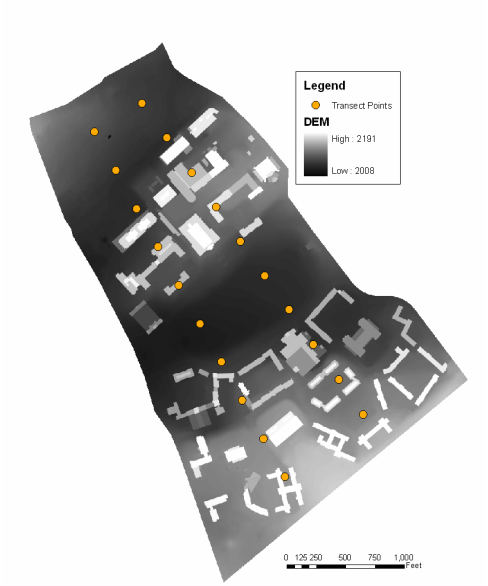

Figure 4.4 – Locations of Transect Sample Points

Another 30 sample points were used in the stratified sample, but viewshed computations were substantially different from that of the random and transect points, as it was desirable to segregate the campus into areas with discrete elevations from those areas with a smoother, more continuous surface to determine if this environment affected the results. A blank polygon shapefile was first added to ArcMap and into this layer seven polygons were digitized to completely cover the study site. The polygons separated the two main classes of elevation data by creating separate pieces whenever a boundary between the classes occurs. The seven areas, together composing the entire study site, were defined as the parking lot adjacent to Prices Fork Road, the academic portion of campus between the parking lot and the Drillfield, the Drillfield

itself, the academic portion of campus between the Drillfield and Washington Street, and the largest three other open spaces: the field near the West Campus Drive and Washington Street intersection, the open space between Dietrich Hall and Washington Street, and the area between Lee, Pritchard, New Residence, Peddrew-Yates, and O'Shaggnaussey Halls. The smaller components of the entire campus DEM exhibited greater elevation fluctuations and were more indicative of the environment immediately surrounding any given sample point.

The campus DEM was copied seven times, but each time one of the seven polygon sections divided by elevation differences was used as an analysis mask. This created seven DEMs, each part corresponding to one of the polygons, and when displayed next to each other appeared to be the entire campus DEM. On each of the seven smaller DEMs, the same neighborhood filter as described above was performed to reduce the resolution to five feet. Placement for sample points was achieved such that each of the seven regions received the same proportion of the sample points as that region's area compared to the entire study site. Table 4.1 defines the seven strata, and lists their area and the number of sample points placed in each.

Stratum	Points	Description	Total Area (acres)
1	6	Parking lot	30.81
2	6	Urban	39.09
3	5	Drillfield	31.58
4	10	Urban	63.61
5	1	Field	6.19
6	1	Field	5.01
7	1	Quad	3.25

Table 4.1 – Strata on Campus

Inside each section, points were placed at random using a random number generator. Figure 4.5 shows the strata boundaries and the locations of sample points inside them. The number inside each stratum refers to the corresponding identification in table 4.1. The same basic model of starting viewshed – optimization – optimal viewshed was employed for each of the starting locations in this stratified sample with one major difference: the viewshed

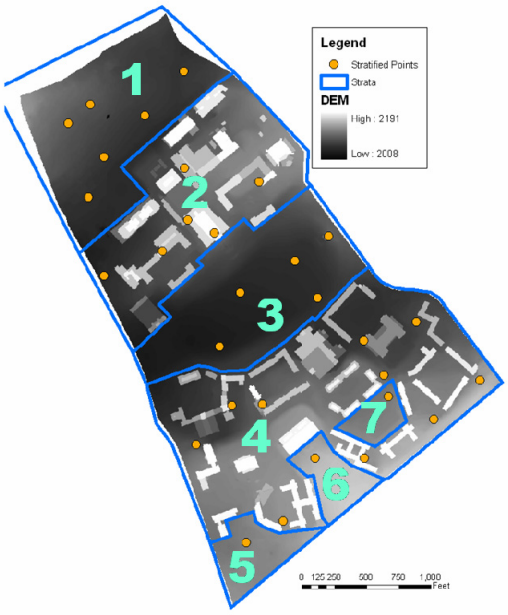

Figure 4.5 – Locations of Stratified Sample Points

for each location was overlaid (multiplication operation) with the polygon boundary of the strata that particular point lies in. This result gave the amount of visible area in just that section of campus rather than the entire study area. All other settings and histogram displays were performed in the same manner as already mentioned.

4.5 – Assumptions

The major assumption made in this research was that the DEM accurately represented the surface. However, a number of sources of error are inherent in transforming any three-dimensional reality to two-dimensional display and study area. While the DEM used in viewshed computations was not free of error, potential sources can be identified and another assumption can be made in that the results achieved from this research with the DEM used would be substantially similar to results from the same experiment using a perfect model.

Good viewing conditions were also assumed; even if the viewshed analysis indicated a point was visible, it may not be at all times. Especially across larger distances, atmospheric effects such as fog or rain can limit visibility. Vegetation, including the presence of trees or shrubs and their related leaf-on / leaf-off seasons, may limit visibility as well. Architecture unique to the Virginia Tech campus such as arches and irregular building surfaces also may contribute to some areas being coded incorrectly in a viewshed analysis. Section 7.1 addresses these issues and how future research can improve the reality of viewshed predictions.

Chapter 5: Results

The ultimate goal of the optimization algorithm is to identify the point in a local neighborhood whose viewshed includes the largest amount of area. Examining the viewsheds of the starting location and the optimal location, as well as their combination, allows for comparison of how well optimization truly met its intended objective.

5.1 – Random Sample Results

The random sample points used should feature no spatial patterns, so their optimization results were expected to demonstrate a strong correlation with difference in elevation of the optimal and initial locations without bias as these relationships include spatial components. The average surface elevation at each of the 30 random starting points was 2062.9 feet, slightly below the average elevation across the entire campus of 2067.5 feet. The highest point before optimization was atop Holden Hall at 2112.1 feet above sea level, while the lowest point was on the western edge of the Drillfield near Davidson Hall, at 2030 feet. The average viewshed for the sample of 30 random starting locations contained 15.3 acres, 8.5% of the total area in the central campus study area (179.6 acres). The random point located atop Eggleston Hall (before optimization) had the largest visible area at 40.3 acres, 22.4% of the area across the entire study site. The starting location between West Campus Drive and Seitz Hall saw the least amount of area at 1.6 acres, only .9% of the campus. The average starting location was 118.9 feet from the nearest building, measured using Euclidian distance from the point to any side of the closest structure. The furthest location from a building was in the northwest corner of the commuter parking lot, 729 feet away from any structure. Five of the thirty starting locations were atop buildings; their distance to the nearest building was assigned 0.

The optimization algorithm was run, obtaining a new network of points on which to conduct visibility analyses. Eight of the thirty random points moved 42.4 feet, the maximum diagonal distance possible from the origin in the 61x61 foot neighborhood in which the optimal location was to be placed. The optimal locations, on average, were 29.2 feet away from their respective original starting locations. These eight points were scattered around campus, and only one of them had a building within the 61x61 neighborhood. The optimal location for two of the thirty random points was the original random location itself, signifying that the random location

yielded the largest viewshed in the local neighborhood. These two points were located at either side of the Drillfield, close to the road which bounds the study site as defined in section 1.4. The average change in elevation from the original location to the optimal location was an increase of 9.1 feet. The largest change in elevation was 52.3 feet, where optimization suggested a move from in front of Patton Hall to on top of the structure. Five of the thirty random points had their optimal locations at the same elevation (and another two as mentioned lie at the exact same location, increasing the total to seven). These points were also distributed across the entire campus. Additionally, there were four optimal points whose location was at a lower elevation, the largest of which was a decrease of 0.9 feet. The four locations were located across campus but were not within the 61x61 neighborhood of a building.

Appendix A provides the initial and optimal locations for each of the sample points, while table 5.1 provides measured and calculated variables for the points in the random sample. Percent gain is defined as the increase in area in relation to the original location; a 100% gain signifies that the optimal viewshed doubled the initial area, a 200% gain represents triple the area, etc. Optimization increased the average elevation of the observer locations to 2072 feet, slightly above the average across the entire campus. The highest optimal location was atop New Residence Hall East at 2124 feet, while the lowest location was 2030 feet, and was the corresponding location of the point whose elevation was lowest prior to running the optimization algorithm. The average viewshed increased to 19.4 acres, 10.8% of the entire campus area. The optimal location with the largest amount of visible area was that point whose original location's viewshed was also the largest; optimization raised this location's viewshed to 42.9 acres (23.9% of the campus). The point atop the rear side of War Memorial Hall presented the smallest viewshed of the optimal locations at 2.4 acres, 1.3% of the campus' total area.

The average optimal viewshed contained 4.1 acres more than that of the average initial location. Optimization for the random location atop Robeson Hall experienced the largest raw increase in area seen, at 26.8 acres, while a point on the Drillfield increased the least at just 0.01 acres. However, when comparing these values to the original starting location, the median point gained 6.21% more area by running the optimization algorithm. Aside from the two points whose optimal location was also the initial location (and thereby did not experience true 'gain' after optimization), each of the remaining points realized some degree of gain after optimization, as hypothesized. The largest gain occurred for a random point alongside Slusher Hall, where the

optimal location moved atop the building and achieved a 649% increase. The smallest amount of gain was 0.02%, at a point located on the Drillfield.

ID	Initial nvis	Initial vis	bld dist	Δ x,y	Δ z	Optimal nvis	Optimal vis	Δ vis	% gain
R1	175.5	4.1	27	42.4	51	151.7	27.8	23.8	585.78
R2	165.2	14.3	146	42.4	0	164.6	14.9	0.6	4.24
R3	154.5	25.1	136	36.1	-0.1	153.4	26.1	1.1	4.28
R4	177.5	2.1	73	36.1	10.3	175.5	4.0	2.0	95.40
R5	174.0	5.5	26	39.1	49.6	166.1	13.5	7.9	142.92
R6	174.1	5.4	0	20.6	0	173.5	6.0	0.6	11.03
R7	157.3	22.2	729	42.4	1.9	157.0	22.5	0.3	1.35
R8	151.0	28.5	138	0.0	0	151.0	28.5	0.0	0.00
R9	161.8	17.8	393	42.4	1.8	160.7	18.8	1.0	5.86
R10	150.6	28.9	409	42.4	0.7	150.4	29.1	0.2	0.68
R11	146.4	33.2	75	26.9	2.1	146.0	33.6	0.4	1.06
R12	176.4	3.2	14	30.4	49.7	165.2	14.4	11.2	351.01
R13	139.3	40.3	0	30.0	0	136.7	42.9	2.6	6.55
R14	149.9	29.6	466	42.4	0.7	149.8	29.8	0.1	0.47
R15	150.2	29.4	132	0.0	0	150.2	29.4	0.0	0.00
R16	151.7	27.9	179	11.2	0.4	151.7	27.9	0.0	0.02
R17	152.4	27.2	13	25.5	52.3	137.4	42.1	14.9	54.87
R18	160.2	19.4	0	20.0	0	159.8	19.8	0.4	2.02
R19	151.7	27.9	39	15.0	-0.4	149.5	30.0	2.2	7.77
R20	175.4	4.2	73	42.4	1.4	174.6	5.0	0.8	19.84
R21	173.7	5.9	47	26.9	-0.9	172.5	7.1	1.2	20.68
R22	175.2	4.4	65	30.0	-0.3	175.2	4.4	0.0	0.98
R23	172.5	7.1	0	10.0	14.2	145.7	33.9	26.8	377.57
R24	176.2	3.4	33	30.0	0.3	175.7	3.9	0.5	14.39
R25	154.1	25.5	75	36.1	0.8	154.0	25.6	0.1	0.26
R26	177.2	2.4	0	11.2	0	177.2	2.4	0.0	1.07
R27	174.7	4.9	126	36.1	-0.5	174.4	5.2	0.3	7.19
R28	178.0	1.6	62	42.4	4.8	169.3	10.3	8.7	544.35
R29	177.2	2.4	21	33.5	32.1	161.6	18.0	15.6	648.86
R30	175.4	4.2	70	31.6	0.1	175.3	4.3	0.1	2.76

Table 5.1 – Results of Random Sample Optimization. The first column identifies the sample point, followed by the amount of not-visible and visible area (measured in acres) in the viewshed of the starting point. The building distance is the distance to the nearest building, Δ x,y is the horizontal distance between the initial and optimal locations, and Δ z is the vertical distance between them, all measured in feet. The following columns give the amount of not-visible and visible area (measured in acres) in the viewshed of the optimal location, and the change in visible area (optimal – initial). The final reported value is the percentage gain, representing optimization.

5.2 – Transect Sample Results

Appendix B provides the initial and optimal locations for each of the sample points in the transect sample, and table 5.2 displays data gathered related to optimization, containing the same information as table 5.1 presents for the random sample. The twenty sample locations evenly distributed along the two transects composed the next set of visibility and optimization analyses. The results are presented here; the values should not be significantly different from those of the other samples, but these points were used for a profile analysis. The sample points were expected to show that optimization was highest at building edges and lowest in open areas because they were placed along lines cutting across the entire campus and therefore assuring coverage of both buildings and open spaces. The average elevation at the starting locations was 2064.3 feet, just below the campus average. Four of the twenty points prior to optimization already were on the top of buildings on campus, with the point at the highest location atop Patton Hall at 2112.1 feet. The lowest starting location was 2031 feet, near the center of the Drillfield. For the transect sample, the average viewshed contained 15.8 acres of visible area (8.8% of the

ID	Initial nvis	Initial vis	bld dist	Δ x,y	Δ z	Optimal nvis	Optimal vis	Δ vis	% gain
T31	155.0	24.6	587	42.4	2.8	153.8	25.8	1.2	4.77
T32	161.9	17.7	310	42.4	1.5	161.1	18.4	0.8	4.27
T33	166.7	12.8	61	30.4	-0.2	166.5	13.1	0.3	2.14
T34	176.7	2.9	0	22.4	0	174.8	4.8	1.9	64.68
T35	139.7	39.8	0	5.0	0	138.9	40.6	0.8	2.04
T36	151.6	28.0	322	42.4	0.9	151.1	28.5	0.5	1.72
T37	145.6	33.9	98	42.4	1.1	145.6	34.0	0.0	0.08
T38	176.3	3.3	6	30.0	25.5	171.6	8.0	4.7	142.89
T39	173.4	6.2	41	39.1	-3	173.0	6.6	0.4	6.17
T40	178.9	0.7	28	39.1	69.7	154.8	24.8	24.1	3423.31
T41	160.8	18.7	406	42.4	0.7	160.0	19.6	0.8	4.54
T42	164.0	15.6	51	39.1	2.4	161.2	18.3	2.7	17.58
T43	176.8	2.7	0	22.4	0	175.7	3.9	1.1	41.34
T44	162.0	17.6	0	42.4	0	159.1	20.5	3.0	16.86
T45	154.6	25.0	38	29.2	-0.4	153.8	25.7	0.7	2.92
T46	151.4	28.2	380	7.1	0	151.3	28.2	0.0	0.14
T47	149.2	30.3	158	42.4	2	148.2	31.4	1.1	3.54
T48	179.3	0.3	11	20.6	21.7	176.1	3.5	3.2	1037.77
T49	177.6	2.0	76	31.6	-0.9	176.9	2.6	0.6	31.37
T50	174.6	5.0	134	0.0	0	174.6	5.0	0.0	0.00

Table 5.2 – Results of Transect Sample Optimization. Table 5.1 provides descriptions of all columns in this table.

entire campus). The point atop Williams Hall had the largest viewshed, 39.8 acres, 22.2% of the total area, while the starting location between War Memorial Hall and Owens Hall had the smallest viewshed at just .3 acres, 0.2% of the central campus. The average starting location was 135 feet from the nearest building; a point in the commuter parking lot was the furthest at 587 feet.

After optimization, the average observer location moved 30.6 feet. Seven of the twenty sample points moved a distance of 42.4 feet; six of these points were either located in the commuter parking lot or the Drillfield. The optimal location within the specified neighborhood for the transect point nearest Lee Hall was the same as the starting location. The average elevation for the network of optimal points was 2070.5 feet, six feet higher than the initial value. The largest change in elevation for the optimal locations was 69.7 feet higher than the original starting location's elevation, and occurred adjacent to Ambler Johnston Hall. There was no change in elevation (from the starting location to optimal location) for five of the twenty points, not including the one location whose optimal spot was the same as the initial. One of these five spots was located in the Drillfield while the other four were atop campus buildings. Four of the starting locations decreased in elevation to the optimal site for observation. All four of these points were in the general vicinity of buildings, but the structures were not within the neighborhood. The largest decrease in elevation was 3 feet and occurred at a location near Dietrich Hall.

The highest optimal location was atop Ambler Johnston Hall, the site of the largest change in elevation, while the lowest optimal elevation was 2031.9 feet, also the spot in the Drillfield with the lowest starting elevation of all transect sample starting locations. However, the largest viewshed among the optimal locations was that atop Williams Hall, and encompassed 40.1 acres of visible area, 22.6% of the entire campus. The average optimal viewshed included 18.2 acres (10.1% of the total area), while the smallest optimal viewshed located near Payne Hall contained 2.6 acres (1.5% of the total area).

The average viewshed of the optimal location contained 2.4 acres more than its respective initial viewshed. The highest raw increase occurred at the point with the largest elevation jump (Ambler Johnston Hall); 24.1 additional acres can be seen. This point also experienced the largest amount of true gain when compared to its initial viewshed, with an astonishing 3423.3% gain in total viewable area. The median point gained 4.66%, while the smallest gain (0.1%) is

achieved at a point on the Drillfield, excluding the one point whose optimal location was also the initial location.

5.3 – Stratified Sample Results

Visibility and optimization processes were also performed across the entire campus DEM for each of the 30 random starting locations in the stratified sample, although visibility statistics are reported only for the area in the stratum in which the point is located. These points in the stratified sample are expected to demonstrate a significant difference in optimization based on their rural or urban environment. Appendix C provides the initial and optimal locations for each of the sample points in the stratified sample, and table 5.3 displays data gathered related to optimization, containing the same information as table 5.1 presents for the random sample.

The average elevation in the northernmost stratum was 2050.8 feet above sea level, while the average change in elevation from the original location to the optimal location was just 1.2 feet. The points were inherently far from any building (average distance was 420 feet) because the strata were separated by their "urban" or "rural" setting. The average viewshed in this stratum contained 17.0 acres, 49.56% of the total area in the section; the range in viewshed size increased from 13.1 acres (38.12%) to 21.6 acres (63.11%). Optimization suggested that the points move an average of 36.6 feet from their initial locations, and increased the average viewshed to 18.0 acres (52.55% of the area). The average location gained 6.72% of area (total range from 0.46% to 17.07%) following optimization.

The average elevation in the next stratum (academic portion of campus) was 2098.1 feet above sea level, and the average elevation of the optimal location was 4.6 feet higher. The points were only 23 feet on average to the nearest building. The average viewshed in this stratum contained 4.6 acres, 11.7% of the total area in the section. The range in the amount of area contained in the viewshed was from .91 acres (2.3%) to 9.9 acres (25.4%). Optimization moved the points an average of 35.9 feet from their initial locations, and increased the average viewshed to 7.1 acres (18.2% of the area). Following optimization, the median location gained 3.80% of area (total range from 2.27% to 598.79%).

The Drillfield stratum's average sample point elevation was 2043.3 feet above sea level, while the average change in elevation from the original location to the optimal location was just 0.5 feet. The sample points were, on average, 308 feet from the nearest building. The average

ID	Initial nvis	Initial vis	bld dist	Δ x,y	Δ z	Optimal nvis	Optimal vis	Δ vis	% gain
S51	12.9	17.9	738	25.0	-1.1	12.8	18.0	0.1	0.46
S52	9.2	21.6	618	25.0	0.0	9.1	21.7	0.1	0.56
S53	12.8	18.0	256	42.4	1.2	11.1	19.7	1.7	9.43
S54	14.9	15.9	222	42.4	1.5	13.6	17.2	1.3	8.19
S55	15.5	15.4	376	42.4	2.1	14.7	16.1	0.7	4.60
S56	17.8	13.1	311	42.4	3.5	15.5	15.3	2.2	17.07
S57	35.6	3.5	97	42.4	-1.6	35.2	3.9	0.4	11.80
S58	37.9	1.2	0	33.5	14.2	30.9	8.2	7.0	598.79
S59	35.1	4.0	0	36.1	0.0	31.8	7.3	3.3	81.24
S60	38.2	0.9	43	35.4	5.3	34.7	4.4	3.5	382.78
S61	29.2	9.9	0	32.0	9.5	28.9	10.2	0.2	2.27
S62	31.2	7.9	0	36.1	0.0	30.4	8.7	0.8	10.12
S63	2.9	28.7	407	39.1	-1.4	2.0	29.6	0.9	3.00
S64	6.5	25.1	403	25.0	0.0	6.4	25.2	0.1	0.38
S65	4.8	26.8	121	42.4	2.2	4.2	27.4	0.6	2.15
S66	4.9	26.7	399	14.1	0.2	4.9	26.7	0.0	0.01
S67	6.4	25.1	209	39.1	1.3	6.3	25.2	0.1	0.45
S68	60.8	2.8	46	33.5	0.9	60.3	3.3	0.5	19.00
S69	61.5	2.2	37	21.2	-0.1	61.4	2.2	0.0	1.12
S70	62.2	1.4	11	30.0	17.8	58.1	5.5	4.1	299.84
S71	56.9	6.7	0	20.0	7.1	54.0	9.6	2.9	43.70
S72	58.3	5.3	48	26.9	-1.5	58.3	5.3	0.0	0.61
S73	59.7	4.0	59	42.4	-3.5	59.6	4.0	0.0	0.35
S74	60.4	3.2	104	42.4	9.4	58.7	4.9	1.7	54.33
S75	61.6	2.0	73	42.4	1.6	61.6	2.0	0.0	2.37
S76	62.7	0.9	37	42.4	0.0	62.5	1.1	0.2	18.48
S77	61.6	2.0	34	42.4	-0.7	61.6	2.0	0.0	0.60
S78	1.7	4.5	162	42.4	1.0	1.3	4.9	0.4	8.36
S79	1.1	3.9	142	42.4	1.5	1.0	4.0	0.1	1.87
S80	0.1	3.1	88	42.4	1.3	0.1	3.1	0.0	0.08

Table 5.3 – Results of Stratified Sample Optimization. Table 5.1 provides descriptions of all columns in this table.

viewshed in this stratum contained 26.5 acres, 83.8% of the total area in the section; the range in viewshed size increased from 25.06 acres (79.4 %) to 28.7 acres (90.9 %). Optimization increased the average viewshed to 26.8 acres (84.9 % of the area) and suggested that the points move an average of 31.9 feet from their initial locations. The average location gained just 1.20% of area (total range from 0.01% to 3%) following optimization.

The average elevation in the southern urban section of campus was 2072.4 feet above sea level, while the average change in elevation from the original location to the optimal location

was 3.1 feet. The points were relatively close to buildings; the average distance was 44 feet. The average viewshed in this stratum contained 3.0 acres, 4.8 % of the total area in the section, and the range in visible area increased from .9 acres (1.4 %) to 6.7 acres (10.5 %). The average location gained 44.04% of area (total range from 0.35% to 299.84%) following optimization. The viewshed optimization algorithm results suggested that the points move an average of 34.4 feet from their initial locations, and increased the average viewshed to 4.0 acres (6.3 % of the area).

Each of the last three strata contained only one sample point each because of their small areas. The sample point in the field near the corner of West Campus Drive and Washington Street was initially located at an elevation of 2078.2 feet; optimization moved the point 42.4 feet and increased the elevation to 2079.2 feet. Its initial viewshed was 4.5 acres (72.3%), and gained 8.36% after optimization to rise to 4.9 acres (79%). The sample point in the field between Dietrich Hall and Washington Street rose 1.5 feet from 2097.9 feet to 2099.4 feet above sea level after optimization, which located the optimal point 42.4 feet away. The viewshed increased from 3.9 acres (78.7%) to 4.0 acres (80.2%). The final sample point, located in the quad to the north of Lee Hall, began at 2067.7 feet of elevation and had a viewshed containing 3.1 acres of visible space inside that stratum, 96.1% of that area. The optimal location for this point was 42.4 feet away, was at an elevation of 2078 feet, and encompassed 3.1 acres (96.2%) in its viewshed.

Chapter 6: Analysis and Discussion

Nearly every variable reported presented a wide range of values, so it is necessary to analyze and discuss why the optimization algorithm performed in the manner it did. Additional calculations are necessary to support the algorithm's decision, and various statistical analyses aid in showing what types of environments are conducive to optimization, and what locations are not.

6.1 – The Random Sample

The random starting location with the highest amount of optimization boasted a gain of 649%, indicating that the optimal location determined by the algorithm saw roughly 7.5 times the amount of area as the initial point. The original location was just 21 feet from Slusher Hall, so its visibility in that direction was immediately limited by the structure. The open area around the point was also limited in size. The optimization algorithm determined the best location was 34 feet away, on the top of the building. Figure 6.1, showing the initial (a) and optimal (b) viewsheds clearly depict why the optimal location is substantially better-suited for placement of

Figure 6.1 (a) – Viewshed Prior to Optimization for Sample Point R29

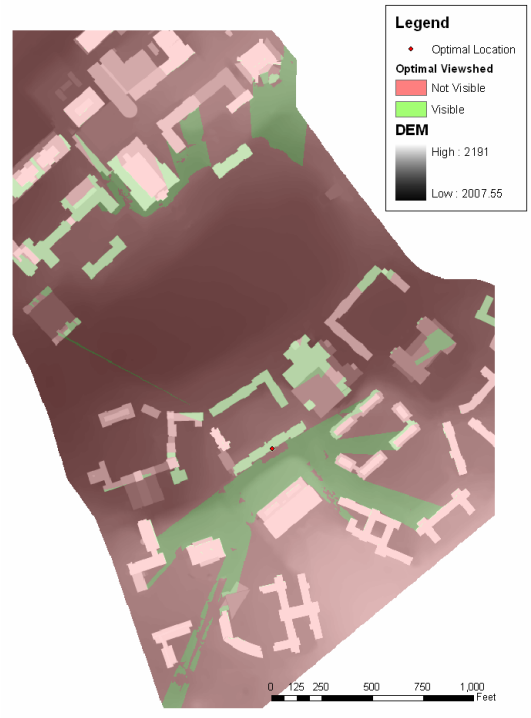

Figure 6.1 (b) – Viewshed After Optimization for Sample Point R29

the observation tower. Visible area is green in both figures.

While the mean optimization rate for the 30 points in the random sample was 97% gain, only six points had optimal locations whose gain is greater; the optimal viewsheds for these cells resulted in 143% - 649% gain. Simple examination of these random samples showed that these six locations all have something in common: their local neighborhood included some part of a building. To test whether or not this relationship is significantly valid, its sample correlation coefficient was computed. Pearson's *r* measures the degree of linear relationship between two variables, and its values range from -1 (perfect negative correlation) to 1 (perfect positive correlation). It is calculated using the formula $r = \frac{S_{XY}}{S_X S_Y}$ where $S_{XY} = \frac{\sum[(X - \overline{X})(Y - \overline{Y})]}{n-1}$, n is the number of observations, S is the sample standard deviation for each variable, and x and y are the two variables for which to test correlation. However, the correlation statistic is highly affected by outlying data; with such a large range in percentage gain, many observations in this viewshed study can be considered outliers. A more meaningful statistic is the population correlation coefficient, ρ, which is a parameter using *r* as an estimate for the population. The null hypothesis (no correlation between the two variables) can be rejected if the test statistic, $t = \frac{r\sqrt{n-2}}{\sqrt{1-r^2}}$ is greater than the critical *t* value from a *t* distribution table with $df = n - 2$ (Schulman 2003).

Based on the statistics presented in table 6.1, there is enough evidence to reject the null hypothesis with 99% confidence and conclude that change in elevation and amount of optimization are positively correlated. As an optimal location moves higher in elevation, a larger increase in the viewshed can be expected. The *r* value of .54 is not extremely strong because several initial locations are actually higher than their optimal locations. However, when the optimal location's elevation was lower than the original starting point, the average gain was only 9.98% of the initial viewshed.

Variable *x*	Change in elevation
Variable *y*	Percent gain
r	0.54
t	3.41
Critical *t* at *c* = .99	2.76

Table 6.1 – Correlation and Significance

Using the same procedure, distance to a building and percentage gain also exhibit a relationship, although the confidence level is less at 75%, and the correlation is not exceptionally strong at -.22 (statistics displayed in table 6.2). Their correlation is negative because as distance to the nearest building (from the initial location) increases, large amounts of optimization decrease, as the algorithm cannot take advantage of larger viewsheds by placing the observation location atop the building. Another test for correlation failed to show statistical significance; the relationship between how far the optimal location is from the initial location and percentage gain experience an *r* value of .07. This value is not alarming, because the amount of optimization is not necessarily expected to be highest at the extreme edges of the neighborhood: some initial locations and optimal locations are the same point, but other optimal locations are far away from their initial point.

Variable *x*	Distance to building
Variable *y*	Percent gain
r	-0.22
t	-1.19
Critical *t* at *c* = .75	-1.18

Table 6.2 – Correlation and Significance

6.2 – The Transect Sample

Data collection and processing for the twenty points located along two transects was performed in the same method as for the random sample, yet a different type of analysis is possible with the transect sample. While it is still important to examine correlation between various measured variables, the random sample has already demonstrated significant relationships, and with the sample size, the same relationships should hold true for the points in the transect sample. However, because the transect points were placed at predetermined, meaningful locations, a different type of data analysis can be performed to show relationships between surface elevation and optimization. Profile graphs are typically reserved for diagramming elevation over distance. On the x-axis, distance is represented, starting at the left from a defined starting location, and increasing to the right until a final destination is reached. On the y-axis, a measured variable is plotted, and increases upward. Two following figures (6.3 and 6.5) show two variables each: optimization improvement (measured by percent gain at each sample point) (displayed in red), and elevation from the DEM (displayed in blue). Horizontally, distance along the transect is shown beginning at the northern end and increasing to the southern end. The names of buildings on campus are included to indicate peaks along the surface

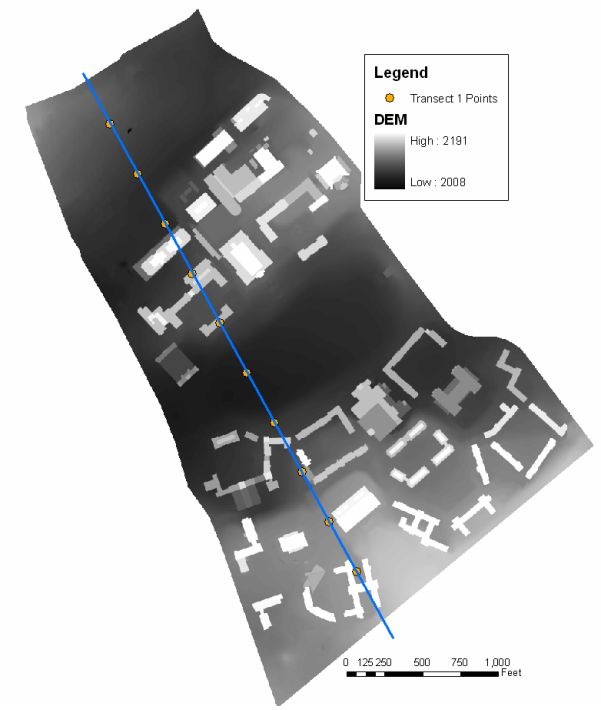

Figure 6.2 – Location of Transect 1

elevation profile. It is important to note that optimization and elevation were measured in different scales, so the two values for a particular distance should not be compared between each other. Rather, the location and steepness of slopes of each curve in relation to one another yields more meaningful discussion. As each transect only contained ten sample points, the profile graphs appeared quite crude, so several other points (along with their optimization values) were added at inflection point locations to produce an accurate depiction. A Kriging interpolation method created a raster surface for optimization, on which ArcGIS' 3D Analyst Extension was used to draw the profiles.

Figure 6.2 shows the ten sample locations and the transect along which they lie. Moving along transect 1 (figure 6.3) from its origin in the commuter parking lot, elevation slightly yet steadily decreases until it becomes flat about 500 feet before Derring Hall. Over the same distance, optimization levels remain steady and very low: in this large and open parking lot, no

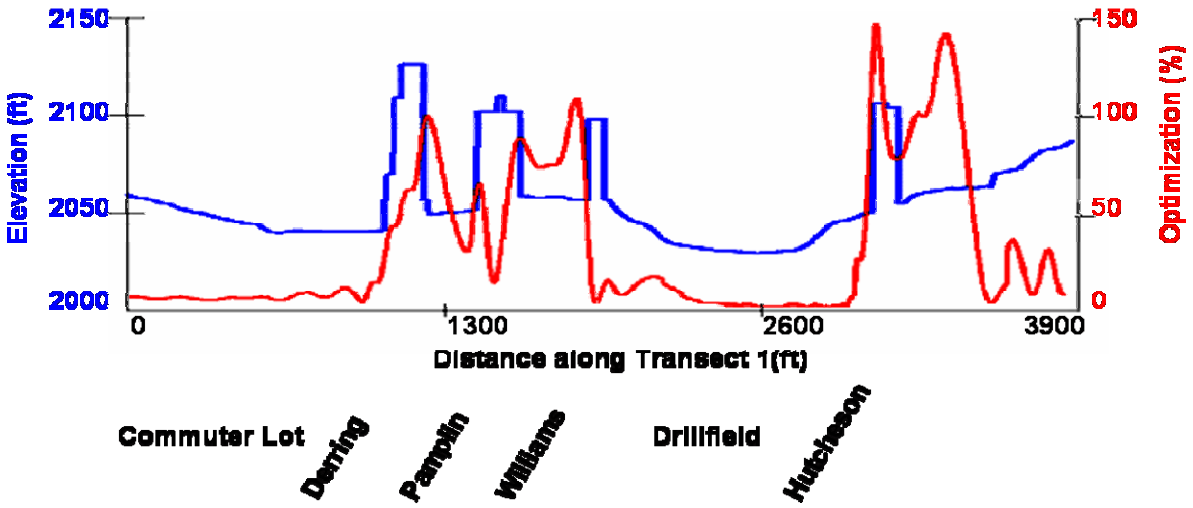

Figure 6.3 – Profile Analysis for Transect 1

one location is likely to realize significant optimization if it is in the neighborhood as the initial point, because both locations almost certainly contain the same area in their viewsheds.

As the elevation profile ascends upon the first spike representing Derring Hall, the percentage gain line rises as well, representing large amounts of optimization possible when a point with a building in its neighborhood has its optimal location atop the structure. Optimization has a local maximum at the same point where the elevation sharply falls from the top of Derring Hall back to the surface. The percentage gain spikes at this location because cells on this side of the building can be optimized at a very high level by moving atop the building. Moving away from Derring Hall, optimization dips to low values, as no location in an area surrounded by buildings is better for an optimal location than another. Optimization then sharply rises as the elevation profile crosses Pamplin Hall, identifying high percentage gain in the area within the 30 foot neighborhood of a building. At the top of Pamplin Hall, optimization dips low again because areas atop the building already have large viewsheds and the algorithm cannot find a significantly better location for observation. High rates of optimization are achieved on the Drillfield-facing side of Pamplin Hall as any cell within the neighborhood of the building has large amounts of percentage gain as the optimal location moves vertically. Optimization then dips and is steady in a small open area but again rapidly increases while the elevation profile approaches Williams Hall. Atop this building, optimization dips as no spot on the building's roof is much better for increasing the viewshed than any other place. Unlike other buildings where optimization sharply rises as elevation values fall back down to the surface, the percentage gain at the front of Williams Hall remains very low, because directly in front of the building, a particular cell can see almost the entire Drillfield, and a spot on the edge of the roof of Williams Hall affords no large amount of optimization.

Both elevation and optimization profiles reach their lowest values crossing the Drillfield. Rates of optimization remain low until the Drillfield is crossed, as most points in this area can see the entire Drillfield, and moving the location of the observer does little to increase viewsheds. As the elevation prepares to climb Hutcheson Hall, optimization sharply rises to its highest point. Locations on the top of this building have extremely large viewsheds as they cover the Drillfield, but because of the slope in front of the building, they cannot view nearly as much. Optimization dips approaching the rear of Hutcheson Hall as its bi-leveled roof shields much of the Drillfield from view. One irregularity in the two variables' relation occurs after the

transect passes Hutcheson Hall as optimization again rises sharply to levels only attained when an observation point is within a neighborhood of a building. While the transect does not cross Slusher Tower, it does come within its local area, so points along the transect can realize large gains in viewshed by having their optimal locations situate atop the building. As the elevation profile nears the southern end of the transect by steadily increasing, optimization rates remain low but fluctuate due to buildings in the general vicinity obstructing viewsheds from particular locations.

Figure 6.4 – Location of Transect 2

The second transect runs roughly parallel to the first and crosses the same type of environments (figure 6.4). Following along the profile analysis (figure 6.5), the transect begins with low and steady elevations in the commuter parking lot, while the optimization rates of this area increases yet still remains low. The optimization rate increases sharply as the surface elevation approaches Whittemore Hall, demonstrating that points within the neighborhood of the building have much larger viewsheds than those areas directly outside of the neighborhood, yet still relatively close to the

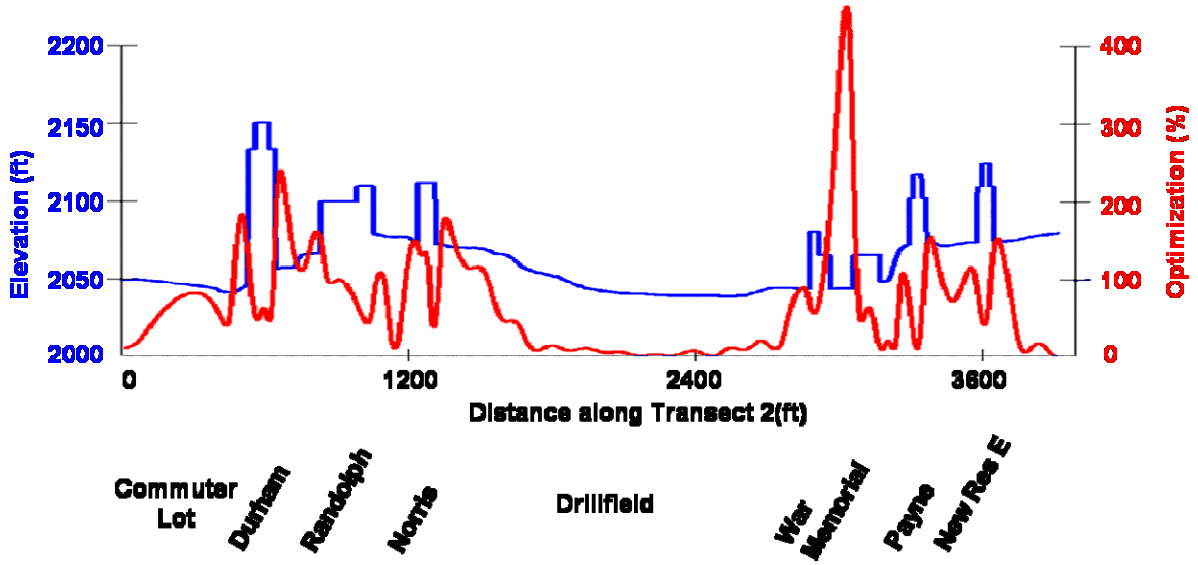

Figure 6.5 – Profile Analysis for Transect 2

building. Atop Whittemore Hall, optimization dips, and beyond it, optimization rises sharply and then falls. This fluctuation repeats itself as the transect crosses Randolph Hall, Norris Hall, War Memorial Hall, Payne Hall, and New Residence Hall East. Between buildings, optimization decreases until arriving at the neighborhood of the next structure, as the open areas typically are enclosed by buildings. Much like the first transect, both optimization and elevation remain very low proceeding across the Drillfield as most locations contain the same viewsheds as their optimal counterpart. The only deviation from these trends in the second transect is in the area of War Memorial Hall. As the transect crosses this building, the elevation plummets to the surface afterward but is in a small nook of the building and crosses it again. However, because this niche is so small, optimization rates ascend to their highest values along the transect as large percentage gains are obtained because the entire area is within the neighborhood of War Memorial Hall. The second transect ends with steady elevation and low optimization values.

While the two transects cross campus in different areas and intersect different features, observation of both elevation and optimization rates yields similar results. In open areas, such as the commuter parking lot, Drillfield, and larger fields between buildings, elevation is expectedly flat while optimization rates may fluctuate but remain at their lowest values. While approaching or leaving the neighborhood of campus buildings, optimization rates tend to increase very sharply as optimal locations are found atop the buildings, yielding much larger percentage gains. While the elevation crosses a building, optimization dips to lower levels because most areas atop the building contain the same large viewshed, and no optimal location is significantly better than the initial position. These trends, repeated several times across each transect, demonstrate that urban areas experience much higher optimization rates than flat and open regions.

6.3 – The Stratified Sample

Viewsheds and LoS analyses were conducted differently for the thirty points in the stratified sample as they were performed only on their respective strata of the DEM, effectively creating distinct environments representative of urban and rural environments. Each of the seven sections of campus was similar within itself, but in a different pseudo-environment than its neighbor. Spatial autocorrelation is a spatial statistic which compares how similar neighboring areas are to one another by measuring the relationship between a variable and itself over distance. Moran's I, ranging from -1 to 1, indicates the degree of spatial autocorrelation.

Regions with areas very similar to their neighbors have a Moran's I value approaching 1, while areas with dissimilar typically experience Moran's I values approaching -1. An area with random values located next to one another should have a Moran's I value near 0.

Stratum	Description	Moran's I
1	Parking lot	0.990
2	Urban	0.324
3	Drillfield	0.997
4	Urban	0.517
5	Field	0.998
6	Field	0.995
7	Quad	0.991

Table 6.3 – Spatial Autocorrelation

To calculate spatial autocorrelation based on elevation for the seven strata of campus, separated by presence or absence of large, open spaces, each the campus DEM and shapefiles of each section were converted for use in IDRISI Andes, an educational software package reserved for raster operations. The Moran's I value for each section is reported in table 6.3.

The five sections of campus featuring open, flat areas all have Moran's I values very near 1. Most locations are inherently very similar to their neighbors as elevation is a continuous surface. The remaining two sections of campus (representative of village or urban spaces) have much lower spatial autocorrelation values. Many points in these areas are similar to their neighbors, but locations along building edges are very dissimilar to others immediately adjacent. Elevation data with fine resolution should feature a very high degree of spatial autocorrelation, which is true in the open sections of campus. However, areas with short term variation lower the spatial autocorrelation values not because across the region the surface value is similar, but rather because there are open areas between buildings alongside pixels that can differ from their neighbor by as much as 120 feet.

Spatial autocorrelation indicates two distinct groups of campus strata are present: five of the seven sections have Moran's I values near 1 (14 observation points), while the remaining two have much lower values (16 observation points). Using optimization values, a *t*-test can be performed with two groups to determine whether or not they are statistically different. The *t*-test must be performed assuming unequal variances, as the two groups do not have the same number of members, and their average optimization values are dissimilar.

The null hypothesis of H_0: $\mu 1 - \mu_2 = 0$ can be rejected if the calculated *t* statistic is within the critical region. This hypothesis states that no difference between the two samples exists. Using the optimization values for the locations in open areas as one sample, and optimization

values for points in the urban portion of campus as the other, the *t* statistic is calculated using the formula $t = \frac{(M_1 - M_2) - (\mu_1 - \mu_2)}{\sqrt{\frac{S_p^2}{n_1} + \frac{S_p^2}{n_2}}}$ in which $S_p^2 = \frac{SS_1 + SS_2}{df_1 + df_2}$, *M* is the mean for each sample, $\mu 1 - \mu_2 = 0$, *n* is the number of observations in each sample, *SS* is the sum of squares for each sample, and *df* is the degrees of freedom for each sample (Gravetter and Wallnau 2004). Table 6.4 provides the statistics indicating that with 28 degrees of freedom ($df = df_1 + df_2$), the null hypothesis can be rejected at $c = .9$. Specifically, viewshed observation points separated by the type of their environment (urban or rural) are concluded to be statistically distinct with 90% confidence.

Group 1	Strata 1, 3, 5, 6, 7
Group 2	Strata 2, 4
t	1.95
Critical *t* at *c* = .9	1.70

Table 6.4 – 2 Sample *t*-test

Separating the observation locations into groups based on the spatial autocorrelation of their region indeed shows that the groups are different, but further analysis of the relationship between Moran's I values and optimization rates reveals the correlation $r = -.42$: as spatial autocorrelation increases (more open area), optimization decreases, which is expected. Table 6.5 provides the necessary statistics to demonstrate that with 95% confidence it can be assured that the data provide enough evidence to conclude that spatial autocorrelation and optimization are negatively related. This means that in areas of high spatial autocorrelation, such as the Drillfield or other large, open areas, optimization values are relatively low. Similarly, in urban environments (areas exhibiting lower spatial autocorrelation), optimization can be achieved at a higher rate, typically by increasing the observer's elevation over short distances.

Variable *x*	Spatial Autocorrelation
Variable *y*	Percent gain
r	-0.42
t	-2.45
Critical *t* at *c* = .95	-2.05

Table 6.5 – Correlation and Significance

In his accuracy analysis in 1991, Fisher mentions spatial autocorrelation as an important consideration and concludes that as Moran's I values increase, the viewshed is more representative. Therefore, the more open sections of campus may have more accurate visibility statistics as there are no large buildings or other obstructions in these strata.

6.4 – Additional Analysis

It is both important and significant to report that all 80 starting locations tested, across all three samples, experienced some degree of gain in their viewshed area after running the optimization algorithm. It is theoretically possible for optimization to reduce the viewshed area because the optimization program chooses only a sample of cells for which to test visibility. Although conducting 30 LoS analyses for each point in the neighborhood should reduce the chance of having no optimization, the potential exists that any given cell in the neighborhood with a true viewshed smaller than the sample point is chosen as a more optimal location based on the specific random points chosen for LoS analysis. Nevertheless, optimization did result in a gain for all sample points, aside from those who did not experience gain because the optimal location was the starting location itself. It is also possible for the same reasons, that other points in the local neighborhood may have a larger viewshed than the point designated as the optimal location, although by sampling theory any point with a viewshed substantially larger than another should have proportionally more of the random points chosen for analysis in its neighborhood. However, this can only be verified through testing the viewsheds of every point in the neighborhood, which is both very time consuming and not necessary, as the identified optimal location still is representative of a location in the neighborhood with a larger viewshed than the initial starting point.

It is also necessary to justify the values for some of the parameters used. The five foot resolution DEM was used solely to improve processing time in the viewshed optimization algorithm. However, as a decrease in resolution can introduce more error and less certainty about the results, three points used in the study (R4, T33, and S71) were chosen at random to be optimized using both one and five foot resolution DEMs. Table 6.6 shows that the viewshed optimization algorithm takes on average 2 minutes 16 seconds to determine an optimal location when using the five foot resolution DEM, but requires 7 hours 56 minutes on average to run over

	R4		T33		S71	
	5 foot DEM	**1 foot DEM**	**5 foot DEM**	**1 foot DEM**	**5 foot DEM**	**1 foot DEM**
Initial Location	(512,666)	(2560,3332)	(371,295)	(1855,1474)	(723,522)	(3615,2610)
Optimal Location	(506,662)	(2531,3311)	(365,296)	(1825,1483)	(723,518)	(3616,2591)
Optimal Viewshed	4.08 acres	4.03 acres	13.11 acres	13.11 acres	9.59 acres	9.60 acres
Processing Time	2m 14s	7h 21m	2m 1s	8h 59m	2m 33s	7h 31m

Table 6.6 – Viewshed Results and Processing Time for Each DEM

the DEM with one foot resolution. Table 6.6 also reports the amount of visible area in the optimal location's viewshed, measured in acres; the tremendous increase in time only results in an average gain of 0.02 more acres visible, less than .4% more for each point tested. Given the substantially insignificant change in optimization values but astonishing processing time increases, it cannot be reasonably justified to use the DEM with one foot resolution when the other is available.

Table 6.7 demonstrates that changing the number of random points for which to test LoS visibility does not greatly impact the amount of visible area in the viewshed of the optimal location. Two points were chosen (one on the Drillfield (T36), and one in a section with buildings (T44)) to test the effect of this parameter. The viewshed optimization algorithm was run ten times on each of these points, changing only the number of random points, whose values were 10, 20, 30….100. Table 6.7 reports the optimal location chosen each time, as well as the amount of visible area in the viewshed from that optimal point. The values where the number of random points tested is 30 are the same values as used in the analysis of all data in previous chapters. The optimal location chosen was not always the same in each run, although there was little fluctuation: five times out of the twenty it was different. However, even though the location of the optimal point changed, the amount of visible area in its viewshed was consistent; out of all twenty runs, the maximum change for the viewshed was 0.05%.

	T36 - (479,491)		T44 - (506,292)	
Random Points	**Optimal Location**	**Optimal Viewshed**	**Optimal Location**	**Optimal Viewshed**
10	(473,497)	28.467	(512,286)	20.509
20	(485,485)	28.473	(512,286)	20.509
30	(485,485)	28.473	(512,286)	20.509
40	(485,485)	28.473	(512,286)	20.509
50	(483,485)	28.466	(512,290)	20.499
60	(485,485)	28.473	(512,286)	20.509
70	(485,485)	28.473	(511,286)	20.502
80	(473,497)	28.467	(512,286)	20.509
90	(485,485)	28.473	(512,286)	20.509
100	(485,485)	28.473	(512,286)	20.509

Table 6.7 – Effect of Number of Random Points on Optimal Viewsheds

Chapter 7: Conclusion

7.1 – Considerations for Further Research

Several other questions may arise from the results of this research. One issue that can continuously be improved is the reality of the DEM. The model used for this research is not perfect, and contains several sources of known and unknown errors. A better DEM could possibly alter the original based on some of the assumptions made, or even eliminate them. Atmospheric conditions affecting visibility could be predicted and the maximum viewing distance reduced. Even a near flawless DEM would be limited by only having one value at any particular cell and being unable to model gaps or other non-uniform distributions.

Related to the reality of the DEM is the difficult concept of modeling an open campus environment. With so many students, faculty, and staff constantly on or in transit to campus, the region is never the same. A large group of students in the Drillfield can certainly obstruct areas beyond it, just as a car in a parking lot can shield its immediate vicinity. Many variables such as people or vehicles are dynamic populations, further complicating their ability to be modeled as they constantly can have different locations. This research does not take these factors into account, so it is apparent that the optimization improvement is for what a camera or sensor can potentially see, but not always what it does see.

Due to their difficulty in being modeled, several other phenomena were assumed to either not be present or not have an impact on all viewsheds when in reality they certainly can affect visibility. The distinction of things that are always non visible from conditions that render an area non visible is another area for potential research. For example, a building will always obstruct area behind it, but trees reduce visibility by blocking some areas behind the tree, although in leaf-off season that area might be visible. Air quality in urban environments might be saturated with smog which restricts visibility that the algorithm would not have noted, just as dense fog does. However, if the fog were to lift, or the smog was clearer one day, the viewshed algorithm may be correct. These conditions may not be able to be modeled in the DEM but rather adjusted for in the algorithm by decreasing the random search distance to test LoS visibility to closer points.

Future research can attempt to add more realism to not only the model but the algorithm itself as well. Cameras, sensors, or other types of observers have properties that can limit or

expand their viewshed as well. Tilting angles, ability to rotate, and zoom capability are examples of potential sources for widening or restricting the field of vision and therefore changing the viewshed. Additionally, this viewshed optimization research was performed with a direct link to visual surveillance. The monitoring of noise, video, or seismic activity also can be explored to determine how the program could be modified to compare other outputs besides traditional viewsheds.

Testing of the algorithm in other regions would also be beneficial even though it should inherently function in any space. The Virginia Tech campus is such a relatively small geographic place, so the same experiment could be investigated in many different environments, for example those that include large areas of water or very mountainous terrain. Tests of how resolution affects the results would also be of interest as repeating a similar study over a much larger area would also require consideration of earth curvature. While the parameters can certainly change among different experiments, they should remain constant in any one study so that results are meaningful when compared at different locations.

7.2 – Application to Designing a Network

One additional aspect to be considered is the establishment of a network of observers instead of iterating this procedure for one at a time. Each LoS and viewshed analysis in this experiment was conducted independent of the others, which does solve the problem of identifying areas that can be seen from one location. However, to ensure adequate surveillance of a sensitive facility, many cameras or sensors would be required. Overlap statistics become more pertinent as too much overlap creates unnecessary redundancy. Similarly, a certain amount of overlap may be desired because in a surveillance or security application, camera malfunction may occur, temporarily rendering one area uncovered. Additionally, the camera network may be the target for destruction of those whom it is trying to identify.

Several previous studies have suggested means for placement of these observers. One such experiment tessellates an area, and adds one camera to each tessellated piece. Visibility is then computed for each camera in the region to determine how many polygons each adequately covers. The camera with the highest rank is added, and then the procedure is iterated until all areas are within view of one camera (Fleishman et al. 2000).

However, studies such as that by Fleishman do not address the issue of optimizing the viewshed. A new method for beginning to establish a network of observers will start with a number of predefined observers and distribute them evenly over a regular grid encompassing the study area. The viewsheds are computed, and the viewshed optimization algorithm is run for each of the points. The neighborhood should be substantially larger than that used in this thesis because it is now desirable to optimize over the entire region instead of one particular location. Unlike a small area such as Virginia Tech's central campus, in a larger region, a starting point has its optimal location relatively far away, it may be sufficient so long as the optimal location adds area not visible to other observers. Any observer who is dominated by another as discussed in section 2.3 is not necessary and can be removed from the network. Finally, additional observers can be sited if there are still large gaps in the area that are not within view of any observer.

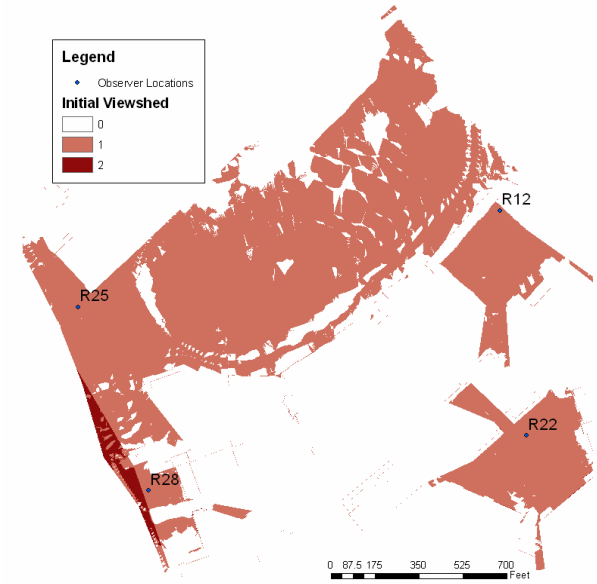

Figure 7.1 (a) – Sample of Network Prior to Optimization

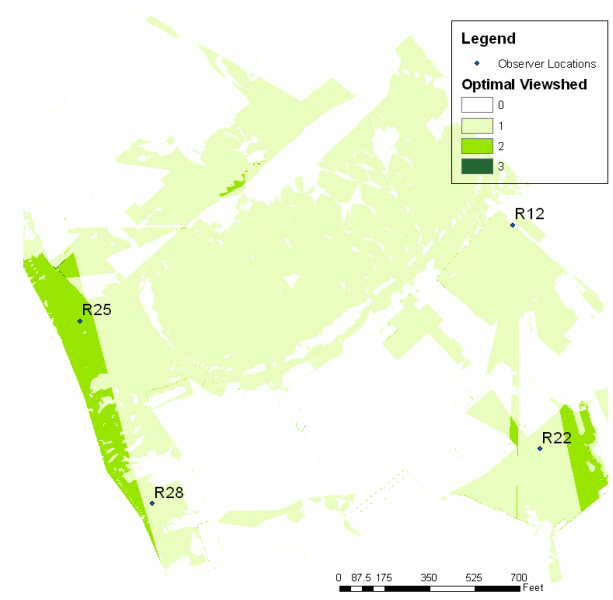

Figure 7.1 (b) – Sample of Network After Optimization

To briefly demonstrate how this methodology might assist in establishing a network of cameras, four points from the random sample were chosen (R12, R22, R25, R28) because they form a rough grid. Their initial viewsheds are overlaid onto each other (addition operation) (figure 7.1

(a)) to demonstrate areas of overlap and no coverage. Darker colors indicate more observers can see that location. Optimization is run on each of them individually, but figure 7.1 (b) shows how much how much more area the entire network can cover. There is substantial overlap between points R25 and R28 but neither dominate each other as they both also cover much area not included in the overlap. It would be necessary to site a new observer in between R22 and R28 as this large area is not covered by any sensor. It may be nearly impossible to attain 100% coverage (Fleishman et al. 2000) without running the optimization algorithm, consequently it would be of interest to modify the program considering overlap from neighboring cameras and analyze its results over a network. The results of an experiment such as this should demonstrate a unique way to establish a network of observers by adding or subtracting individual ones when necessary. Rather than optimizing the entire network which would be extremely iterative, this method ensures adequate coverage because each of the observers in the network is known to be optimized and cannot cover any more area in its local neighborhood. With this tool, an experienced surveillance designer could more quickly and effectively design protection for a sensitive location.

7.3 - Summary

The viewshed optimization algorithm succeeds in its intended role of serving as a user-friendly tool aiding in the placement of observation locations for viewshed analyses. Those points selected for the random sample demonstrate a positive relationship between vertical distance change (optimal elevation – initial elevation) and amount of optimization. The transect sample shows what types of areas experience the smallest and largest gains in visible area: areas alongside buildings have the potential to increase their optimization by as much as 3,400% by choosing the optimal location to be atop that building. Flatter areas, such as parking lots, open fields, or large rooftops do not encounter much optimization at all, as their neighbors are more likely to contain the same amount of area in their viewshed. When the campus is split into two strata based on common spatial autocorrelation values, there is a significant difference of the optimization values.

The results have demonstrated that in order to optimize the amount of visible area in an urban environment, or one with rapidly changing elevation, the optimal placement for observation is at higher elevation. While tremendous optimization values are not realized in

open or more continuous settings, the viewshed optimization algorithm typically finds a better location. Contrary to common thought, this optimal spot is not always at the highest elevation in the neighborhood: several initial locations experience the largest optimization gain when moved to a lower elevation. This tool, while not yet commercially packaged in the GIS industry's leading software, is certainly a valuable component to any viewshed analysis.

Literature Cited

Booth, Bob. Using ArcGIS 3D Analyst. GIS by ESRI. Redlands, CA: Environmental Systems Research Institute, Inc. 2000.

Bresenham, J.E. Algorithm for computer control of a digital plotter. IBM Systems Journal. Vol. 4, No. 1. 1965: 25-30.

Fisher, Peter. Algorithm and Implementation Uncertainty in Viewshed Analysis. International Journal of Geographic Information Systems. Vol. 7, No. 4. 1993: 331-347.

Fisher, Peter. First Experiments in Viewshed Uncertainty: Simulating Fuzzy Viewsheds. Photogrammetric Engineering & Remote Sensing. Vol. 58, No. 3. 1992: 345-352.

Fisher, Peter. First Experiments in Viewshed Uncertainty: The Accuracy of the Viewshed Area. Photogrammetric Engineering & Remote Sensing. Vol. 57, No. 10. 1991: 1321-1327.

Fleishman, Shachar, Cohen-Or, Daniel, and Lischinski, Dani. Automatic Camera Placement for Image-Based Modeling. Computer Graphics Forum. Vol. 19, No. 2. 2000: 101-110.

Franklin, W. Randolph, and Vogt, Christian. Multiple Observer Siting on Terrain with Intervisibility or Lo-Res Data. Presented at ISPRS Congress, Istanbul, Turkey, July 2004. 6pp. Accessed online at <http://www.isprs.org/istanbul2004/comm7/papers/229.pdf>.

Germroth, Matthew. GIS and Satellite Visibility: Viewsheds from Space. Master's Thesis, Virginia Tech, 2005. 92 pages.

Gravetter, Frederick, and Wallnau, Larry. Statistics for the Behavioral Sciences, Sixth Edition. Belmont, CA: Thomson Learning. 746 pages.

Kidner, David, Sparkes, Andrew, Dorey, Mark, Ware, J. Mark, and Jones, Christopher. Visibility Analysis with the Multiscale Implicit TIN. Transactions in GIS. Vol. 5, No. 1. 2001: 19-37.

Lam, Nina Siu-Ngan, and Quattrochi, Dale. On the Issues of Scale, Resolution, and Fractal Analysis in the Mapping Sciences. The Professional Geographer. Vol. 44, No. 1. 1992: 88-98.

Lee, Jay. Digital Analysis of Viewshed Inclusion and Topographic Features on Digital Elevation Models. Photogrammetric Engineering & Remote Sensing. Vol. 60, No. 4. 1994: 451-456.

Monckton, Colin G. An Investigation into the spatial structure of error in digital elevation data. Innovations in GIS. Edited by Michael Worboys. London: Taylor & Francis. 1995: 201-211.

Nackaerts, Kris, Govers, Gerard, and Van Orshoven, Jos. Accuracy Assessment of Probabilistic Visibilities. International Journal of Geographic Information Science. Vol. 13, No. 7. 1999: 709-721.

Ruiz, Marilyn. A causal analysis of error in viewsheds from USGS digital elevation models. Transactions in GIS. Vol. 2, No. 1. 1997: 85-94.

Schulman, Robert. Lecture Notes: Statistics 3604. Spring 2003, Virginia Tech.

Sorensen, Paul, and Lanter, David. Two Algorithms for Determining Partial Visibility and Reducing Data Structure Induced Error in Viewshed Analysis. Photogrammetric Engineering & Remote Sensing. Vol. 59, No. 7. 1993: 1149-1160.

Tobler, Waldo. A computer model simulation of urban growth in the Detroit region. Economic Geography, Vol. 46 (Supplement Proceedings). 1970: 234-240.

Virginia Tech. High-Res Main Campus Map. Accessed online at <http://www.vt.edu/where_we_are/maps/documents/vt_main_map.pdf>.

Wang, Jianjun, Robinson, Gary, and White, Kevin. A Fast Solution to Local Viewshed Computation Using Grid-Based Digital Elevation Models. Photogrammetric Engineering & Remote Sensing. Vol. 62, No. 10. 1996: 1157-1164.

Watson, D.F., and Philip, G.M. A Refinement of Inverse Distance Weighted Interpolation. Geoprocessing. Vol 2. 1985: 315-327.

Appendix A

Raw Data for Random Sample:

ID	Initial i	Initial j	Initial z (ft)	Optimal i	Optimal j	Optimal z (ft)
R1	678	485	2044.0	672	491	2095.0
R2	340	301	2040.0	334	295	2040.0
R3	409	597	2035.0	413	591	2034.9
R4	512	666	2048.3	506	662	2058.6
R5	750	601	2074.4	745	595	2124.0
R6	453	233	2100.0	454	229	2100.0
R7	270	204	2059.0	264	198	2060.9
R8	400	536	2030.0	400	536	2030.0
R9	329	237	2044.4	323	231	2046.2
R10	521	489	2032.8	527	483	2033.5
R11	506	378	2059.1	504	373	2061.2
R12	715	444	2045.3	721	445	2095.0
R13	670	479	2095.0	670	473	2095.0
R14	560	441	2037.5	566	435	2038.2
R15	670	334	2064.0	670	334	2064.0
R16	577	372	2045.2	576	370	2045.6
R17	569	336	2056.4	568	331	2108.7
R18	510	283	2112.1	510	287	2112.1
R19	611	526	2046.8	608	526	2046.4
R20	666	784	2101.4	672	778	2102.8
R21	848	550	2068.6	846	545	2067.7
R22	737	624	2074.3	731	624	2074.0
R23	400	387	2101.8	402	387	2116.0
R24	669	610	2072.1	663	610	2072.4
R25	380	521	2030.1	386	525	2030.9
R26	650	556	2085.0	648	555	2085.0
R27	589	717	2084.5	583	713	2084.0
R28	436	668	2050.4	430	674	2055.2
R29	602	619	2071.9	605	613	2104.0
R30	483	766	2078.0	481	760	2078.1

Appendix B

Raw Data for Transect Sample:

ID	Initial i	Initial j	Initial z (ft)	Optimal i	Optimal j	Optimal z (ft)
T31	299	164	2059.6	293	158	2062.4
T32	335	229	2044.5	329	223	2046.0
T33	371	295	2040.5	365	296	2040.3
T34	407	360	2101.8	409	356	2101.8
T35	443	426	2098.0	444	426	2098.0
T36	479	491	2031.0	485	485	2031.9
T37	515	557	2045.8	521	563	2046.9
T38	551	622	2062.0	557	622	2087.5
T39	587	688	2086.8	582	682	2083.8
T40	623	754	2086.3	617	749	2156.0
T41	380	115	2049.0	374	121	2049.7
T42	422	174	2041.0	416	169	2043.4
T43	464	234	2100.0	462	230	2100.0
T44	506	292	2112.1	512	286	2112.1
T45	548	351	2054.0	545	356	2053.6
T46	589	410	2039.9	590	411	2039.9
T47	631	468	2039.0	637	474	2041.0
T48	673	527	2043.6	672	531	2065.3
T49	715	588	2071.7	709	590	2070.8
T50	757	646	2079.0	757	646	2079.0

Appendix C

Raw Data for Stratified Sample:

ID	Initial i	Initial j	Initial z (ft)	Optimal i	Optimal j	Optimal z (ft)
S51	262	183	2063.2	266	186	2062.1
S52	296	154	2062.4	299	150	2062.4
S53	442	102	2046.1	448	108	2047.3
S54	381	171	2045.1	375	165	2046.6
S55	318	236	2046.2	312	230	2048.3
S56	294	298	2041.8	288	292	2045.3
S57	318	421	2040.3	312	415	2038.7
S58	409	383	2101.8	403	386	2116.0
S59	449	334	2109.9	443	330	2109.9
S60	443	253	2099.0	448	248	2104.3
S61	560	274	2113.5	565	278	2123.0
S62	490	354	2124.0	496	350	2124.0
S63	668	359	2066.6	662	364	2065.2
S64	615	397	2041.3	610	397	2041.3
S65	651	456	2041.1	657	462	2043.3
S66	531	448	2036.6	533	446	2036.8
S67	498	531	2030.8	504	536	2032.1
S68	462	685	2058.4	456	682	2059.3
S69	518	624	2052.0	515	621	2051.9
S70	565	621	2067.8	565	627	2085.6
S71	723	522	2079.7	723	518	2086.8
S72	805	493	2054.1	800	495	2052.6
S73	754	576	2066.2	760	570	2062.7
S74	833	645	2086.5	839	651	2095.9
S75	904	584	2088.0	910	578	2089.6
S76	724	706	2085.0	730	700	2085.0
S77	597	804	2086.0	591	798	2085.3
S78	540	837	2078.2	546	831	2079.2
S79	647	706	2097.9	653	712	2099.4
S80	761	609	2076.7	767	615	2078.0

Appendix D

VirginiaTech
Invent the Future

MAIN CAMPUS MAP

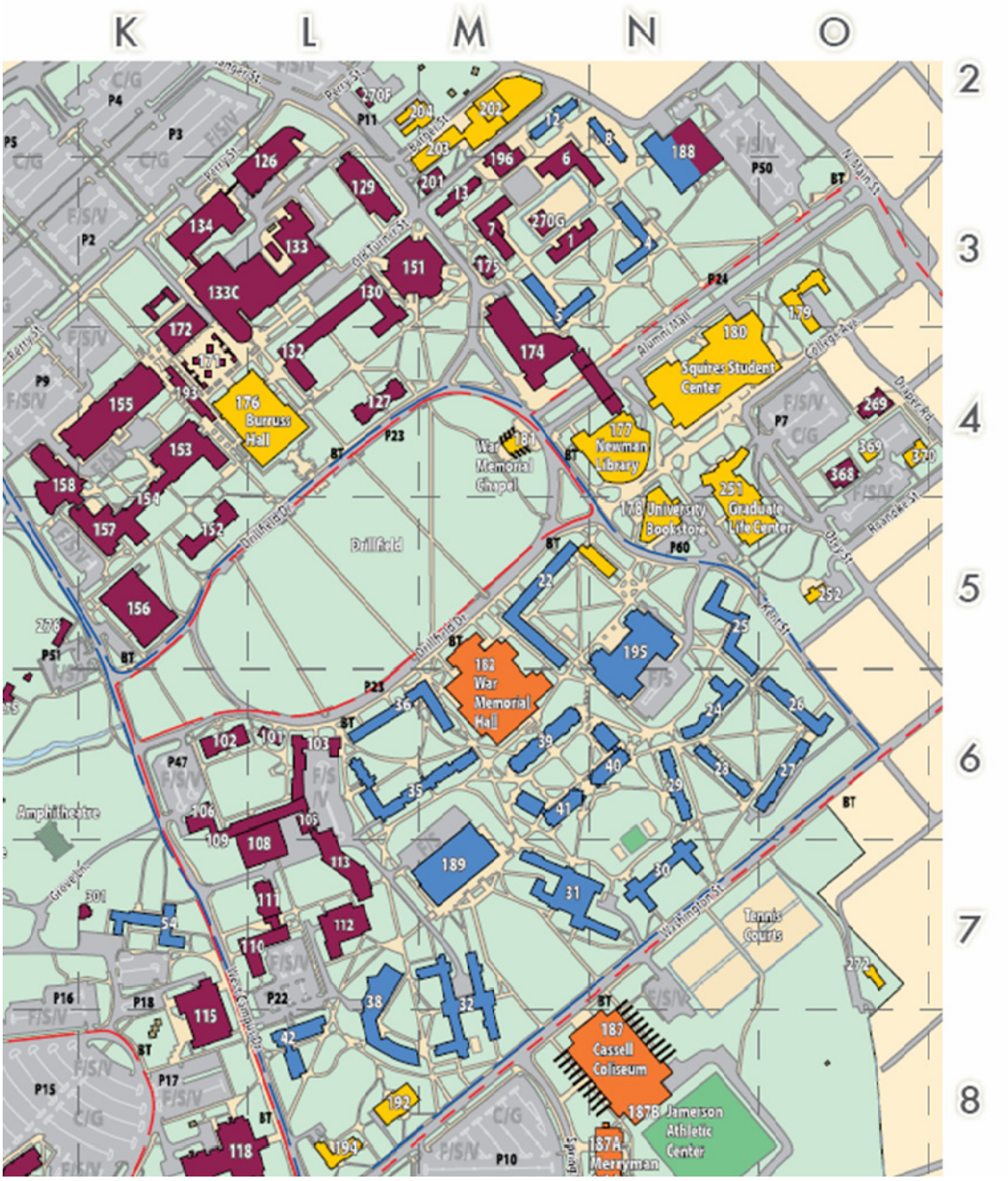

Alphabetical Key for Campus Map

K-7.....109.....Agnew Hall
L-7.....113.....Agriculture/Forestry Research. Laboratory Facility
M-2.....204.....Air Conditioning Facility
M-8.....032.....Ambler Johnston Hall
O-4.....368.....Architecture Annex
O-4.....269.....Armory
M-2.....196.....Art and Design Learning Center
O-6.....026.....Barringer Hall
J-9.....119.....Bioinformatics Phase I
J-9.....120.....Bioinformatics Phase II
M-3.....005.....Brodie Hall
L-2.....270F.....Building 270F
K-4.....171.....Burchard Hall
K-4.....193.....Burke Johnston Student Center
N-12.....183.....Burrows/Burleson Tennis Center
L-4.....176.....Burruss Hall
L-6.....036.....Campbell Hall
L-8.....194.....Career Services Building
N-8.....187.....Cassell Coliseum
Q-10.....241.....Central Stores
L-7.....112.....Cheatham Hall
J-4.....158.....Chemistry/Physics Building
L-8.....038.....Cochrane Hall
M-3.....270G.....College of Science Admin. Bldg.
K-3.....172.....Cowgill Hall
O-7.....272.....Cranwell International Center
J-12.....475.....Dairy Science Complex
K-5.....156.....Davidson Hall
K-4.....155.....Derring Hall
M-7.....189.....Dietrick Hall
L-2.....126.....Durham Hall
M-5.....022.....Eggleston Hall
L-7.....110.....Engel Hall
K-10.....185D.....English Field
M-3.....013.....Femoyer Hall
P-10.....240.....Fleet Services
J-9.....123.....Food Science and Technology
L-7.....111.....Fralin Biotechnology Center
I-5.....295.....Golf Course Clubhouse
O-5.....251.....Graduate Life Center at. Donaldson Brown
L-9.....124.....Greenhouses
J-7.....274.....The Grove
K-5.....157.....Hahn Hall
K-9.....124A.....Hahn Horticulture Gardens
K-3.....133C.....Hancock Hall
L-8.....042.....Harper Hall
I-10.....149C.....Harry T. Peters Large Animal Clinic
N-12.....459.....Health and Safety Building
O-3.....179.....Henderson Hall
K-7.....054.....Hillcrest Hall
L-3.....130.....Holden Hall
I-4.....250C.....Holtzman Alumni Center
L-6.....103.....Hutcheson Hall
N-8.....187B.....Jamerson Athletic Center
N-6.....028.....Johnson Hall
M-3.....001.....Lane Hall
N-9.....185.....Lane Stadium/Worsham Field
N-7.....030.....Lee Hall
K-8.....118.....Litton-Reaves Hall
M-3.....007.....Major Williams Hall
M-3.....151.....McBryde Hall
L-9.....191.....McComas Hall
O-4.....369.....Media Annex
P-4.....370.....Media Building
N-8.....187A.....Merryman Athletic Facility
O-6.....027.....Miles Hall
M-2.....203.....Military Building
N-2.....008.....Monteith Hall
N-6.....040.....New Residence Hall – East
N-6.....024.....Newman Hall
N-4.....177.....Newman Library
L-4.....132.....Norris Hall
M-3.....201.....Old Security Building
N-6.....029.....O'Shaughnessy Hall
N-5.....195.....Owens Hall
K-4.....153.....Pamplin Hall
N-12.....455.....Parking Services
L-4.....127.....Patton Hall
M-6.....039.....Payne Hall
M-6.....041.....Peddrew-Yates Residence Hall
M-3.....175.....Performing Arts Building
P-10.....242.....Police Department
M-2.....202.....Power Plant
K-6.....102.....Price Hall
L-3.....277.....Price House/Women's. Resource Center
M-7.....031.....Pritchard Hall
L-3.....133.....Randolph Hall
N-3.....004.....Rasche Hall
L-10.....186.....Rector Field House
I-11.....149B.....Richard B. Talbot Educational. Resources Center
K-5.....154.....Robeson Hall
L-6.....101.....Sandy Hall
K-6.....106.....Saunders Hall
L-7.....108.....Seitz Hall
N-2.....006.....Shanks Hall
N-2.....188.....Shultz Hall
I-4.....250B.....Skelton Conference Center
M-6.....035.....Slusher Hall
L-3.....356.....Smith House
L-6.....105.....Smyth Hall
J-6.....275.....Solitude
O-10.....190.....Southgate Center
N-4.....180.....Squires Student Center
P-10.....242.....Sterrett Facilities Complex
L-8.....192.....Student Services Building
N-12.....183.....Tennis Center
H-4.....250A.....The Inn at Virginia Tech
M-2.....012.....Thomas Hall
M-4.....174.....Torgersen Hall
N-5.....178.....University Bookstore
O-5.....252.....University Club
N-5.....025.....Vawter Hall
J-11.....149.....Virginia-Maryland Regional. College of Veterinary Medicine
K-12.....313.....Visitor Information Center
K-7.....301.....Wallace Annex
K-8.....115.....Wallace Hall
M-4.....181.....War Memorial Chapel
M-6.....182.....War Memorial Hall
K-3.....134.....Whittemore Hall
J-11.....149A.....William E. Lavery Health. Research Center
K-5.....152.....Williams Hall
M-10.....185H.....Women's Softball Field
J-5.....276.....Wright House

Vita

Benjamin Peter Turko was born in 1983 in Alexandria, Virginia to his parents Peter and Carren Turko. He has two younger brothers, Brian and David. A 2001 graduate of Robinson Secondary School in Fairfax, Virginia, Ben entered Virginia Tech as a freshman in August 2001. During all summer and winter vacations from Virginia Tech, he worked as a Data Technician with Infologics Corporation, a contractor to the United States Department of Transportation in Washington, D.C. He received a BA in Geography (Geospatial and Environmental Analysis option), with minors in Geosciences and Spanish in May 2005.

Ben entered Virginia Tech as a Masters Candidate in the Department of Geography in August 2005. He was a graduate teaching assistant for GEOG 4084: Introduction to GIS, where he was charged with grading tests and projects, and teaching 2 weekly lab sessions for 120 students. Ben became a graduate research assistant in spring 2006, sponsored by Lockheed Martin. He designed and modified computer algorithms to optimize individual cameras and sensors and began working on a project to integrate the ideas into a network. He graduated from Virginia Tech in spring 2007 with an MS in Geography. In June 2007, he began working as a Geospatial Analyst at the National Geospatial-Intelligence Agency upon graduation.